GEORGIA INSTITUTE OF TECHNOLOGY
Engineering Experiment Station
Atlanta, Georgia 30332

FINAL REPORT

PROJECT NO. A-934

MILLIMETER AND SUBMILLIMETER WAVE DIELECTRIC MEASUREMENTS WITH AN INTERFERENCE SPECTROMETER

By

Albert McSweeney and Albert P. Sheppard

CONTRACT Nonr-991(13)

14 April 1970

Performed for

Office of Naval Research
Department of the Navy
Washington, D. C. 20360

PREFACE

This report serves to summarize work accomplished under the subject contract over its duration from 15 April 1966 to 14 April 1970. Several technical papers which describe both the research approach and many of the results obtained therefrom were published during this period. This report is organized so as to summarize the overall view of the program and then to utilize the published papers as appendices to fill in appropriate details. Information on aspects of the research which has not been reported in the open literature is included in the main body of the report.

TABLE OF CONTENTS

LIST OF FIGURES

MILLIMETER AND SUBMILLIMETER WAVE DIELECTRIC MEASUREMENTS WITH AN INTERFERENCE SPECTROMETER

I. Introduction

The extension of laser techniques to the far infrared by Gebbie et al., in 1964 [1], opened some new avenues for applications of this portion of the electromagnetic spectrum. For the first time a coherent source was available which did not have the built-in weaknesses so inherent to microwave tubes as their frequency of oscillation is extended upward. Since 1964, many other laser transitions have been observed and coverage of the 100-1000 μm wavelength region with laser sources is now within the realm of possibilities.

Almost concurrent with the laser frequency extension to the far infrared, liquid helium cooled germanium bolometers were improved so that Low [2] has reported on a unit with sensitivity of 10^{-14} watts/$Hz^{\frac{1}{2}}$. The laser also opens possibilities for superheterodyne detection should applications demand or warrant greater available sensitivity in receivers for the far infrared.

The high-resolution and wide-modulation bandwidths may, of course, be cited as potential advantages for any frequency region, including the far infrared, that is above the presently widely used microwave spectrum. Likewise, components tend to get smaller in volume and lighter in weight as frequency increases.

Component development, however, for this frequency region is very likely to be of a quasi-optical nature which uses prisms, beamsplitters, etc., in

either a free-space transmission mode or in oversize waveguide. In any case, dielectric materials are destined to play an even more important role in submillimeter and far infrared systems than they do in the microwave region.

Because frequency variable coherent sources are not yet available to cover continuously the millimeter and far infrared spectrum, an instrument such as the 30 cm aperture Michelson interference spectrometer available at Georgia Tech [3] provides an excellent means of gathering data on a number of dielectric materials for frequencies from 50 to 3000 GHz (1.67 to 100 cm^{-1}). This report summarizes how this instrument has been used to obtain dielectric constant, loss tangent, and transmission coefficient on materials which have been widely used by the microwave engineer or optical physicist in components, spectroscopy, or overall systems and thus have a high potential for being a logical choice for similar needs that may arise in the 50 to 3000 GHz region.

II. Instrumentation and Measurement Procedure

As described in Technical Report No. 1 on this contract [3] and in the reprint of Appendix A, dielectric constant information can be obtained with the interference spectrometer by first finding the central maximum associated with the zero effective path difference between the two perpendicular mirror arm positions and the spectrometer beamsplitter. Insertion of the dielectric sample to be measured into the optical path of one of these arms causes a phase shift which can be measured by adjusting the movable arm a distance, ΔL, so as to obtain once again a maximum. If the sample has a thickness, d, then

the dielectric constant is

$$\epsilon \simeq \left(1 + \frac{\Delta L}{d}\right)^2 \quad . \tag{1}$$

Appendix A also shows the error in Equation (1) as a function of sample thickness and the magnitude of ϵ. It has been found that for materials with dielectric constant less than about 10, the measurement error resulting from multiple reflections can be easily limited to a value less than 1%.

Loss tangent is determined by inserting the sample between the black body source of the spectrometer and the input collimating optics and obtaining a spectrum. A reference spectrum without the sample is also obtained. The ratio of these spectra yields the transmission coefficient of the sample. If the dielectric constant is known then the loss tangent can be calculated according to Equation (8) in Appendix A. The instrument is used in this mode with a wide resolution bandwidth which averages out the effects of multiple reflections, thus approximating a sample of infinite thickness. The advantages of the approach are that it offers the capability of obtaining data to calculate loss tangent as a function of frequency over a wide frequency band with a single measurement, and that the accuracy of the loss tangent measurements is not radically affected by small uncertainty in the value of relative dielectric constant at a given frequency.

The frequency resolution in interferometer dielectric constant measurements is determined by the frequency response of the beamsplitter and detector, by additional filters placed in the beam, and by the frequency distribution of radiation generated by the source.

Figures 1 and 2 show the frequency response of two different arrangements of the spectrometer. Thus, in order to make relative dielectric constant measurements at a given frequency band it is necessary to select the source, detector, and beamsplitter combination which will limit the detected power to the desired band of frequencies. Additional filters are a better way of limiting the frequency bandwidth to a relatively narrow part of the submillimeter spectrum.

In one approach to filtering the radiation for the dielectric constant measurements, Fabry-Perot filters of the type described by Ulrich, Renk and Genzel [4] were constructed. These consisted of two dimension metal grids separated by a thin dielectric sheet.

The metal grids used were 250, 333, and 500 mesh nickel grids separated by Mylar sheets. Available thicknesses of Mylar are 0.004, 0.002, and 0.0015 inch. These thicknesses allowed filter design center frequencies of 690 GHz (23 cm^{-1}), 1200 GHz (40 cm^{-1}) and 1500 GHz (50 cm^{-1}).

Measurements to determine the properties of a filter using 250 line-per-inch mesh grids separated by a 0.004-inch thick sheet of Mylar yielded a first resonance at 624 GHz (20.8 cm^{-1}), a Q of about 4, and a transmission coefficient at the center of the pass-band of about 0.5. The transmission spectrum of this filter is shown in Figure 3.

Figure 4 shows the transmission curve for a similar filter made with 0.004-inch thick Mylar between sheets of 333 line-per-inch metal mesh. This filter also had a low Q and poor transmission coefficient at the center frequency.

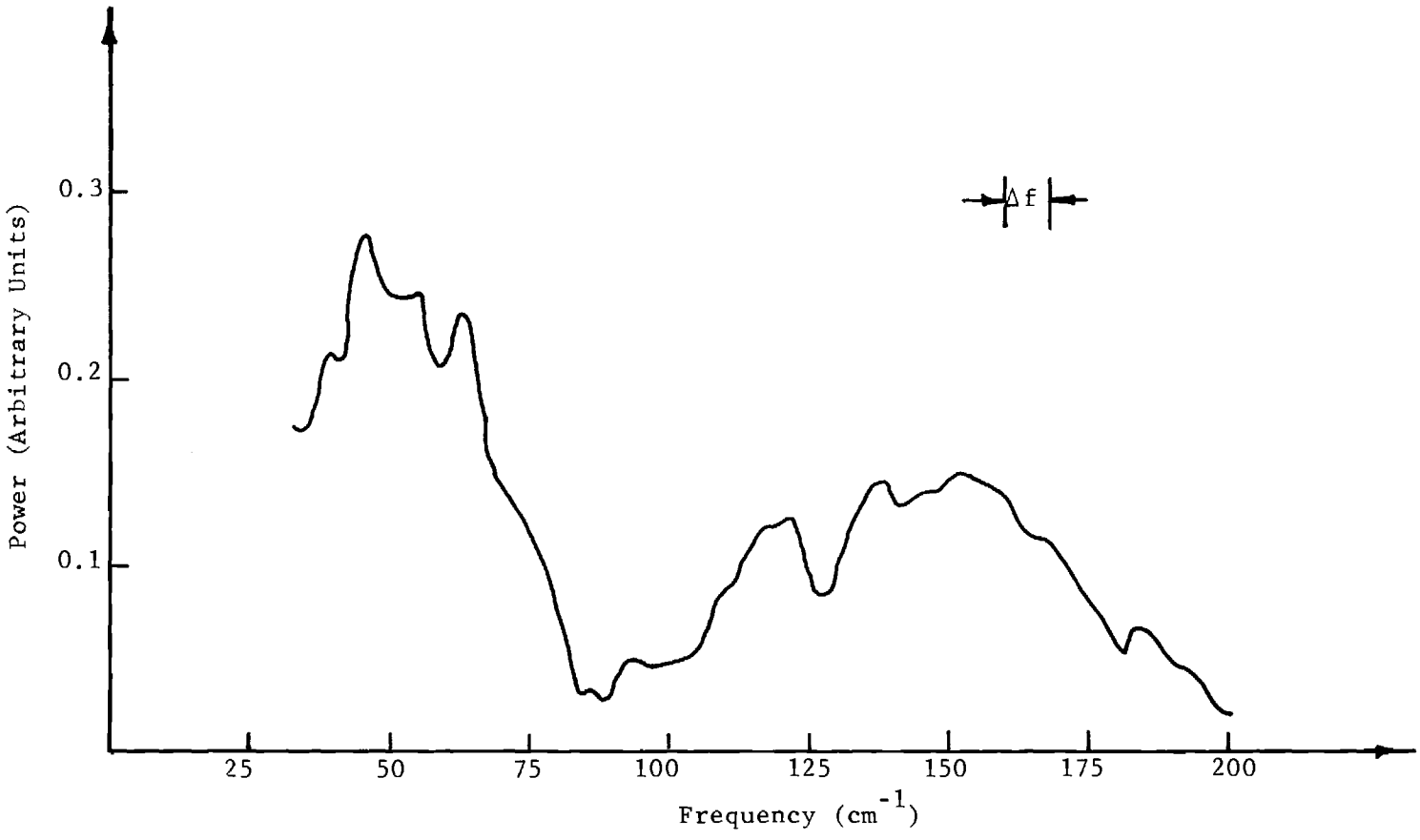

Figure 1. Spectral Bandpass of the Fourier Transform Spectrometer Using Golay Detector, 0.0005" thick Mylar Beamsplitter, and Hg Arc Source.

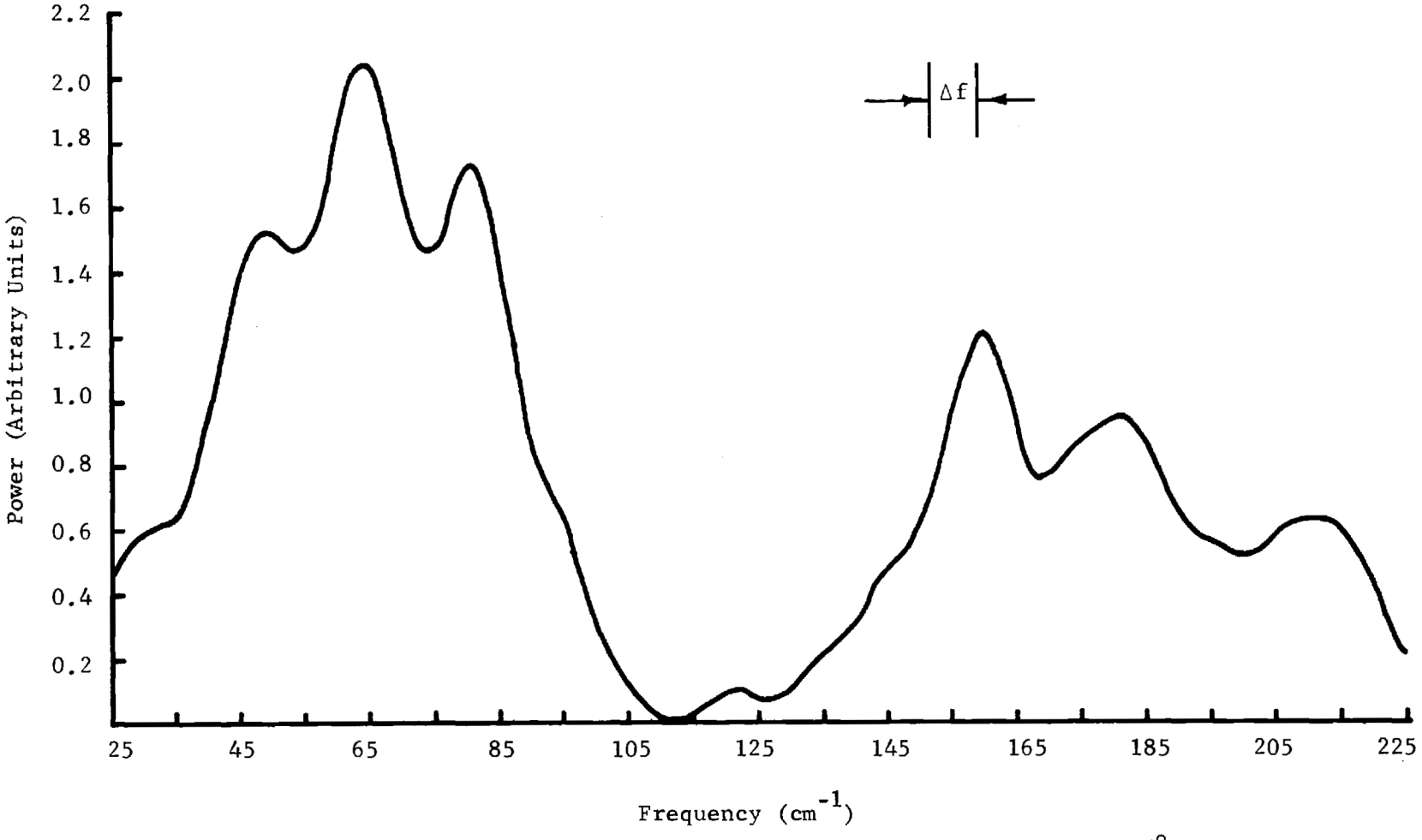

Figure 2. Spectral Bandpass of the Fourier Transform Spectrometer Using 2°K Detector, 0.001" thick Mylar Beamsplitter, and Graphite Oven Source.

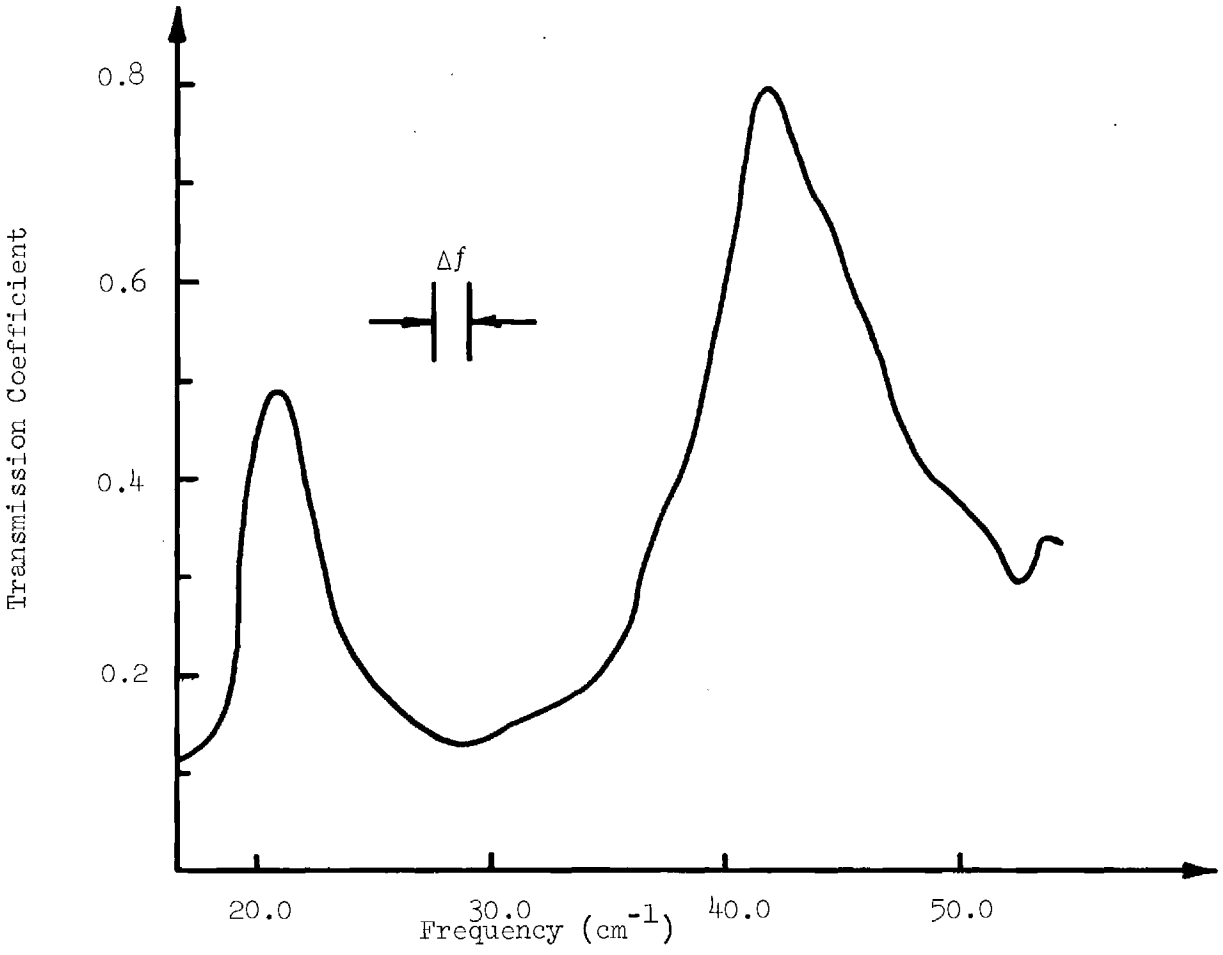

Figure 3. Transmission coefficient vs. frequency for 250-line-per-inch, 0.004 inch thick Fabry-Perot filter.

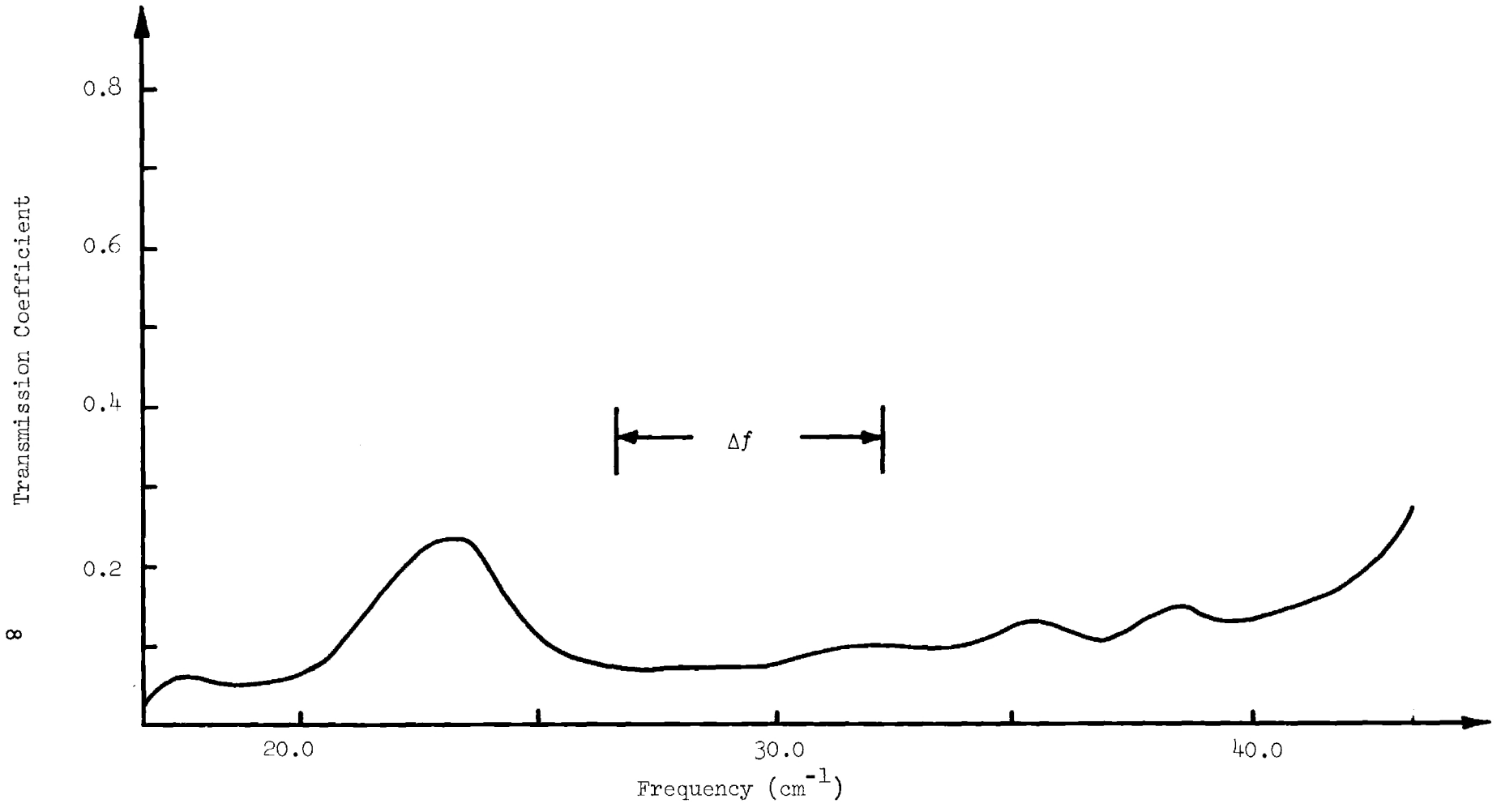

Figure 4. Transmission coefficient vs. frequency for 333-line-per inch, 0.004 inch thick Fabry-Perot filter.

Other filters consisting of different combinations of metal mesh and Mylar thicknesses showed even worse results. The low values of transmission coefficient and Q of these filters can probably be attributed to the high loss of Mylar at these frequencies and to variations in thickness of the Mylar sheets and collodion glue holding the metal grids to the Mylar.

Better results have been obtained with echelette gratings than with the metal grid Fabry-Perot filters. One advantage of these gratings over the filters is that the gratings are reflection rather than transmission devices; consequently, the high insertion loss of the transmission filters discussed earlier is avoided. Also, the reflection gratings are less fragile than are the transmission filters. As a result, the use of echellete gratings was a more efficient technique than the use of Fabry-Perot filters for band-pass filtering in interferometer relative dielectric constant measurements.

Figure 5 is a sketch which illustrates the important parameters of a blazed grating. An expression relating the groove spacing d, the diffraction order m, the effective width of the grating W, and the Q is

$$d = \frac{mW}{Q} \quad , \tag{2}$$

and the blaze angle, θ_B, is calculated from the expression

$$\theta_B = \sin^{-1}\left(\frac{Q\lambda}{2W \cos \theta_i}\right) \quad , \tag{3}$$

where θ_i is the angle between an incident ray and the normal to the wider

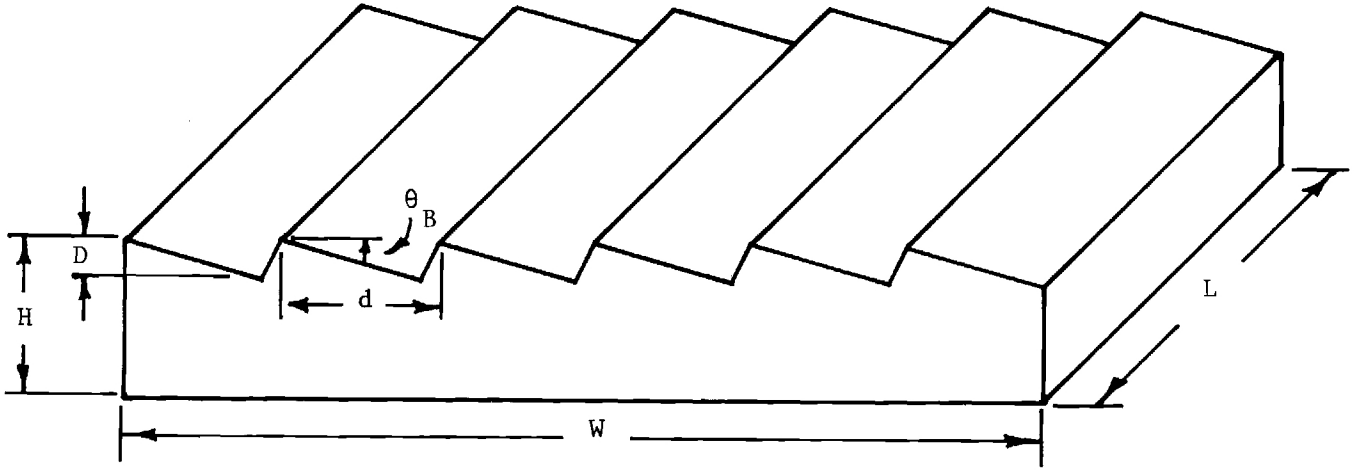

Figure 5. Blazed Grating

surface of the grooves. For specular reflection, the angle of incidence has the same value as the angle of reflection. Therefore, θ_i is chosen to be half the angle between an incident ray and a line from the center of the grating to the center of the next mirror in the optical system.

The groove depth, indicated in Figure 5, is

$$D = d \sin \theta_B \cos \theta_B \quad , \tag{4}$$

assuming a 90° angle between the groove surfaces.

Two frequencies were selected for the design of blazed gratings to be inserted into the Georgia Tech interference spectrometer. One was 80 GHz (26.7 cm^{-1}), which was chosen because of the relatively low absorption by water vapor and because of the liquid helium cooled detector sensitivity at this frequency. The other frequency chosen was 1300 GHz (43.3 cm^{-1}). This is the frequency at which the spectrometer is most sensitive when used in conjunction with the 0.0015-inch beamsplitter, the Golay cell, and the mercury arc lamp.

The gratings were designed to have low Q values in order to maintain a good signal-to-noise ratio. Decreasing the bandwidth of the radiation increases frequency resolution for relative dielectric constant measurements but reduces the amount of energy which reaches the detector. A bandwidth of 90 GHz (3.0 cm^{-1}) was selected as a suitable compromise between frequency resolution and signal-to-noise ratio.

At 26.7 cm^{-1}, the 3.0 cm^{-1} bandwidth implies a Q of 8.9. This value of Q, together with an approximate value of 0.75 inch for the effective beamwidth, substituted into Equation (2), yields a value of d = 0.086 inch for first-order diffraction.

The value of θ_i to be used in Equation (3) for calculating the blaze angle, θ_B, was measured to be 6.5°, based on consideration of an analysis of the angles in the spectrometer input optics.

The values of Q, W, θ_i, and λ at 26.7 cm^{-1} substituted into Equation (3) yield a value of $\theta_B = 5^\circ$.

Equation (4) and the above values for d and θ_B lead to a value of the groove depth D of 0.007 inch to the nearest thousandth of an inch.

Therefore, the machining dimensions for the 26.7 cm^{-1} grating were:

W = 0.75 inch,

d = 0.086 inch,

$\theta_B = 5^\circ$, and

D = 0.007 inch.

By the same process, the machining dimensions for the 43.3 cm^{-1} grating were specified as:

W = 0.75 inch,

d = 0.053 inch,

$\theta_B = 5^\circ$, and

D = 0.005 inch.

The measured bandwidth of these gratings was four and one-half times the predicted value. This probably means that the 0.75-inch value for W, the effective grating width, was far too large. In view of the fact that the detector aperture is of the order of 1/8 inch, this is not surprising.

Two new gratings were constructed with the following parameters:

	26.7 cm^{-1} Grating	43.3 cm^{-1} Grating
W	0.75 in	0.75 in
d	0.019 in	0.012 in
θ_B	23°	23°
D	0.007 in	0.004 in

The above changes in d and θ_B were designed to give a five-to-one increase in the Q of the gratings, and maintain the same center frequencies.

The measured center frequencies of the two gratings are 840 GHz (28 cm^{-1}) and 1320 GHz (44 cm^{-1}). The difference between the actual and the designed center frequencies can probably be attributed to the ± 0.001" tolerance in machining dimensions.

The transmission spectra of these gratings are shown in Figures 6, 7, 8, and 9. From Figure 6, it is seen that the actual Q of the 28 cm^{-1} grating is 6.5. The spectrometer housing and the multi-path auxiliary chamber in which the grating was mounted were both evacuated to less than 0.1 Torr for this measurement. The second order pass-band occurs within the spectrometer pass-band and is seen in the figure at approximately 1560 GHz (52 cm^{-1}).

Figure 7 shows the transmission coefficient vs. frequency for the 28 cm^{-1} grating in the multi-path chamber at atmospheric pressure. The reduced value of the tranmission coefficient of the two pass-bands is caused by absorption of water vapor.

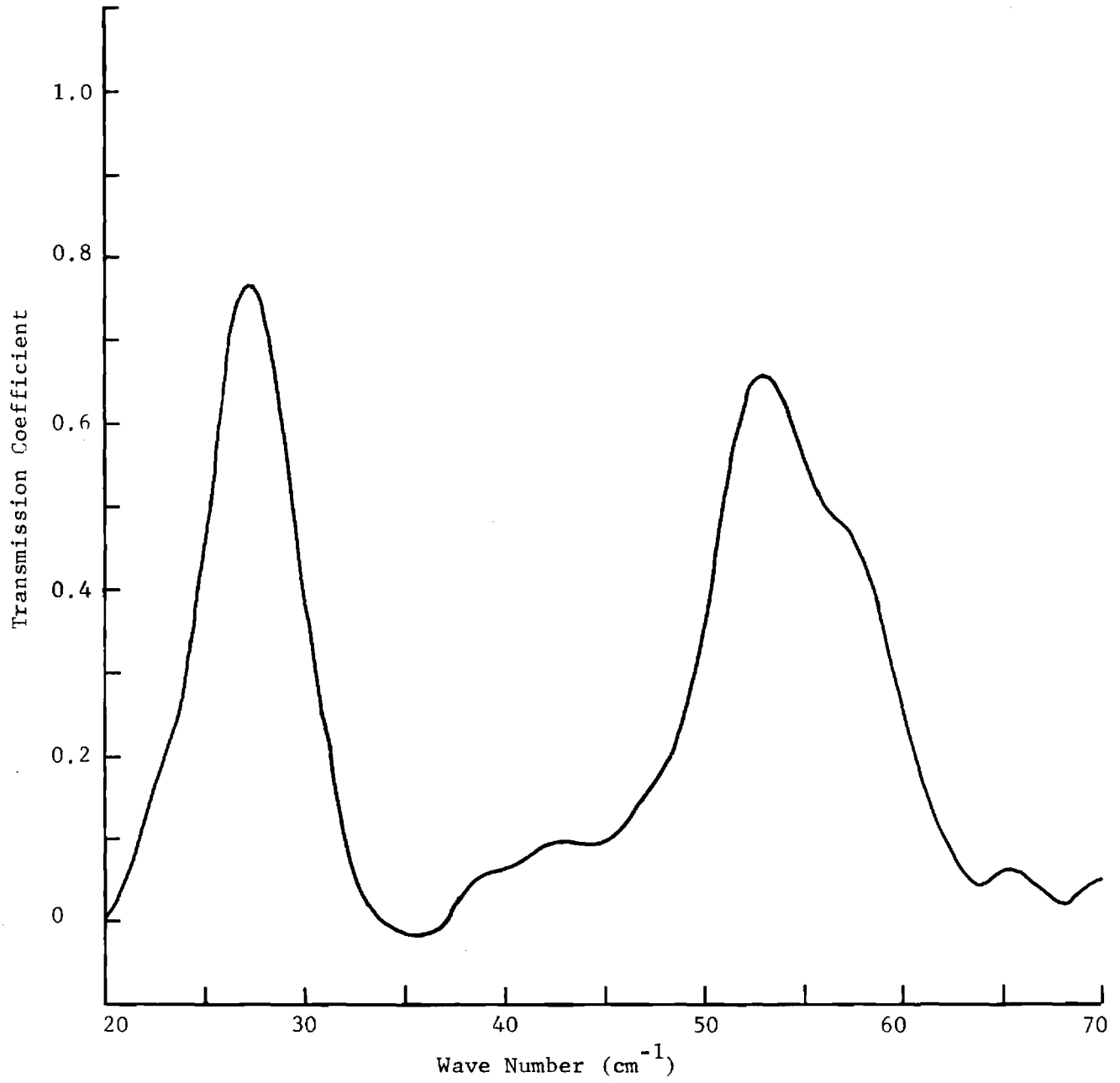

Figure 6. Transmission Spectrum of 28 cm^{-1} Grating in a Vacuum

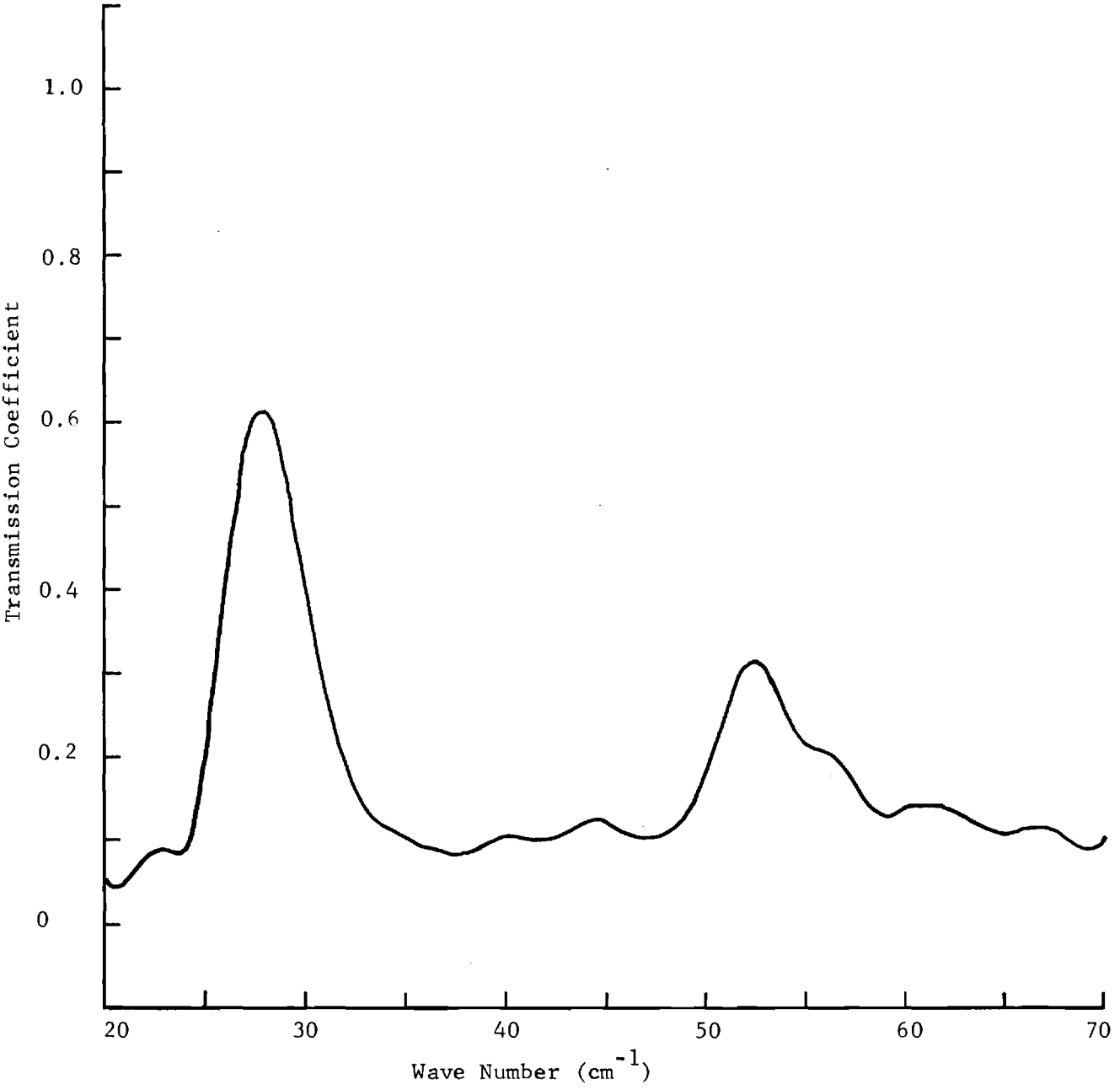

Figure 7. Transmission Spectrum of 28 cm^{-1} Grating in Room Atmospheric Conditions

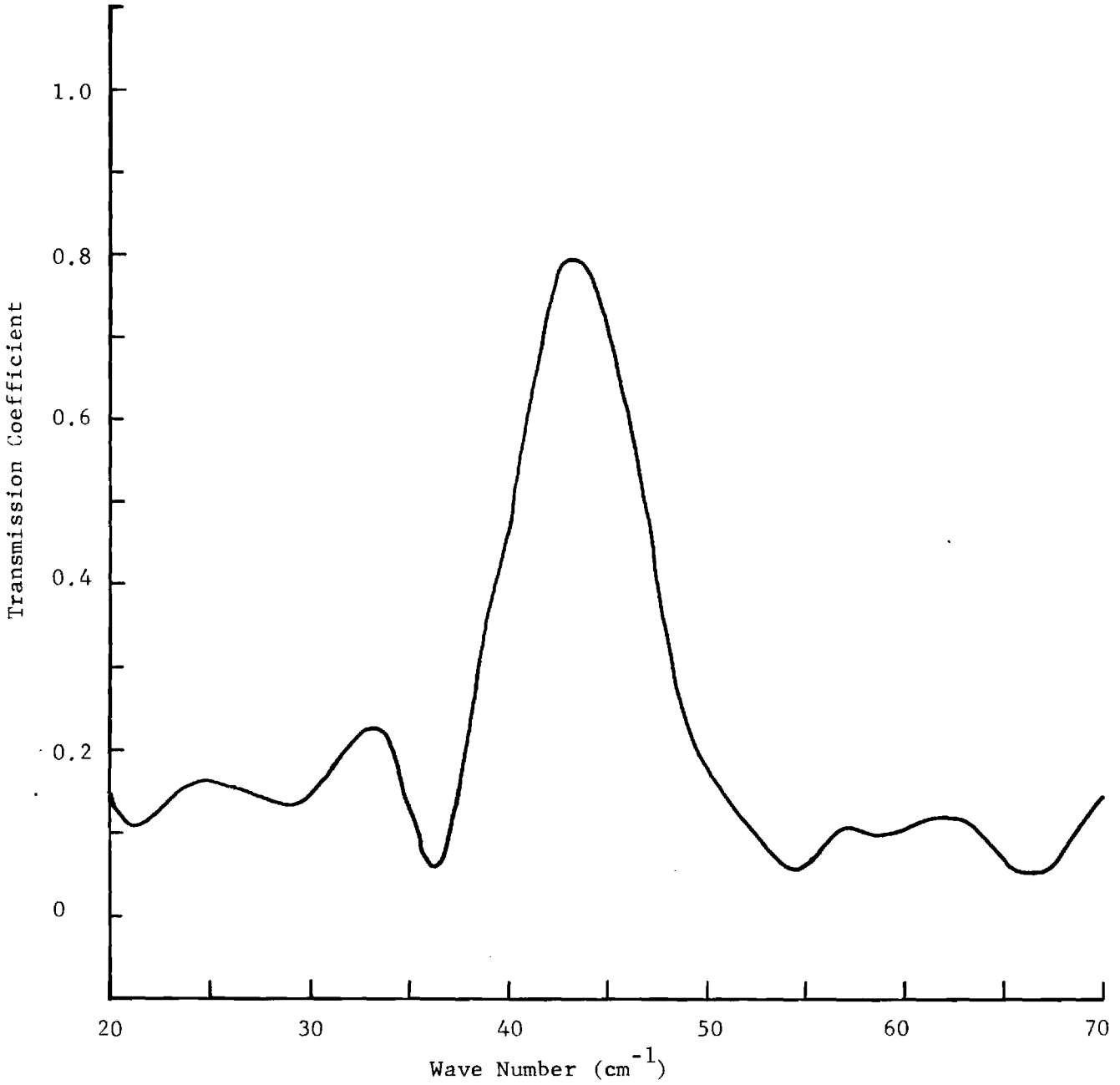

Figure 8. Transmission Spectrum of 44 cm^{-1} Grating in a Vacuum

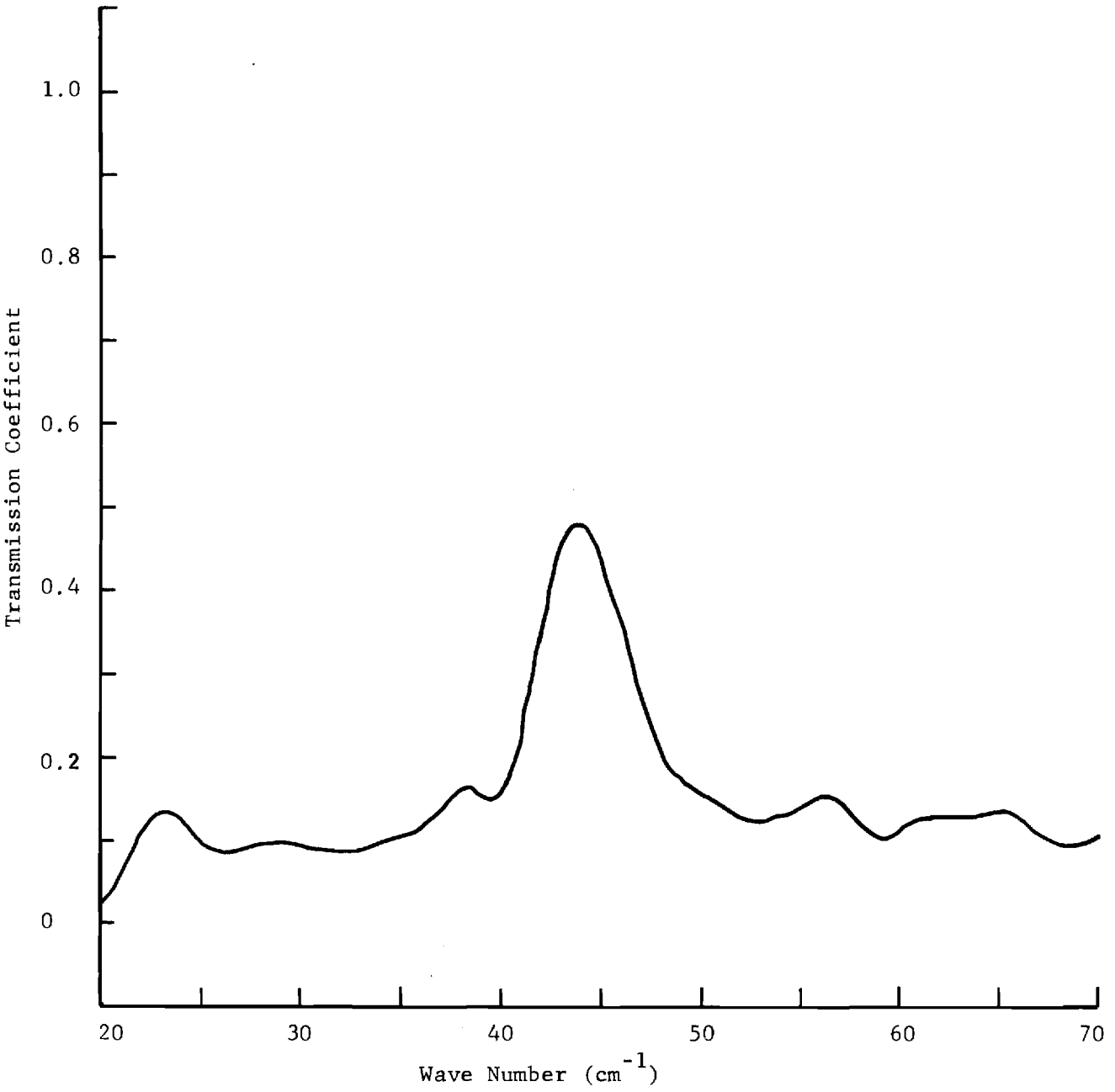

Figure 9. Transmission Spectrum of 44 cm^{-1} Grating in Room Atmospheric Conditions

Figures 8 and 9 are graphs of transmission coefficient vs. frequency for the 44 cm^{-1} grating with the chamber evacuated and at atmospheric pressure, respectively. The second-order pass-band occurs at approximately 2640 GHz (88 cm^{-1}) which is beyond the spectrometer pass-band when using the 0.0015-inch thick beamsplitter. The low value of transmission coefficient in Figure 9 as compared with Figure 8 is again due to absorption by water vapor.

III. Results

The dielectric constant and loss tangent of a large number of dielectric samples were measured in the course of the program. Results of these measurements are tabulated in Appendices A-D. It may be noted that these measurements were improved in accuracy over the duration of the contract as better signal-to-noise ratio was obtained, spectral filters installed, and instrument errors minimized.

As seen in Appendix D transmission coefficients of several materials were also reported. In order to measure dielectric constant accurately, a relatively large diameter sample is required ($\sim$ 10 cm minimum). It becomes very costly to obtain samples of some materials of this diameter whereas samples of 2-3 cm diameter are fairly inexpensive. Thus transmission coefficient data which can be obtained with small diameter samples have been measured. The particular materials measured are sufficiently important as electromagnetic window materials in other parts of the spectrum that it was deemed essential to obtain some data in the submillimeter region. The

transmission coefficient spectrum does show very well the usefulness of a given material as a window or absorber as the case may be. Transmission coefficient spectra on several materials in addition to those reported in Appendix D also were measured. These are shown in Figures 10, 11, 12, 13, and 14.

Most dielectric materials measured show an increasing loss tangent as a function of increasing frequency. Many of the common microwave dielectrics do, however, remain usable to at least 2000 GHz (67 cm^{-1}). Teflon and polyethylene are especially notable in that their loss tangent is very low up to 2000 GHz and only a small change is shown in dielectric constant from the microwave region to 2000 GHz. From a strictly electrical point of view, these two materials are excellent candidates for millimeter and submillimeter wave windows or component parts. Rexolite shows somewhat more of an increase in loss tangent but in view of its excellent mechanical properties also would be an excellent choice of material for millimeter and submillimeter applications. For higher temperature applications, slip-cast fused silica will serve with sufficiently low loss to be a satisfactory window material or component part.

IV. Other Aspects of the Research

Apart from the main line of measurements reported above and in the attached Appendices, other techniques were explored which would provide more insight into measurement procedures for obtaining accurate millimeter and submillimeter wave dielectric materials data.

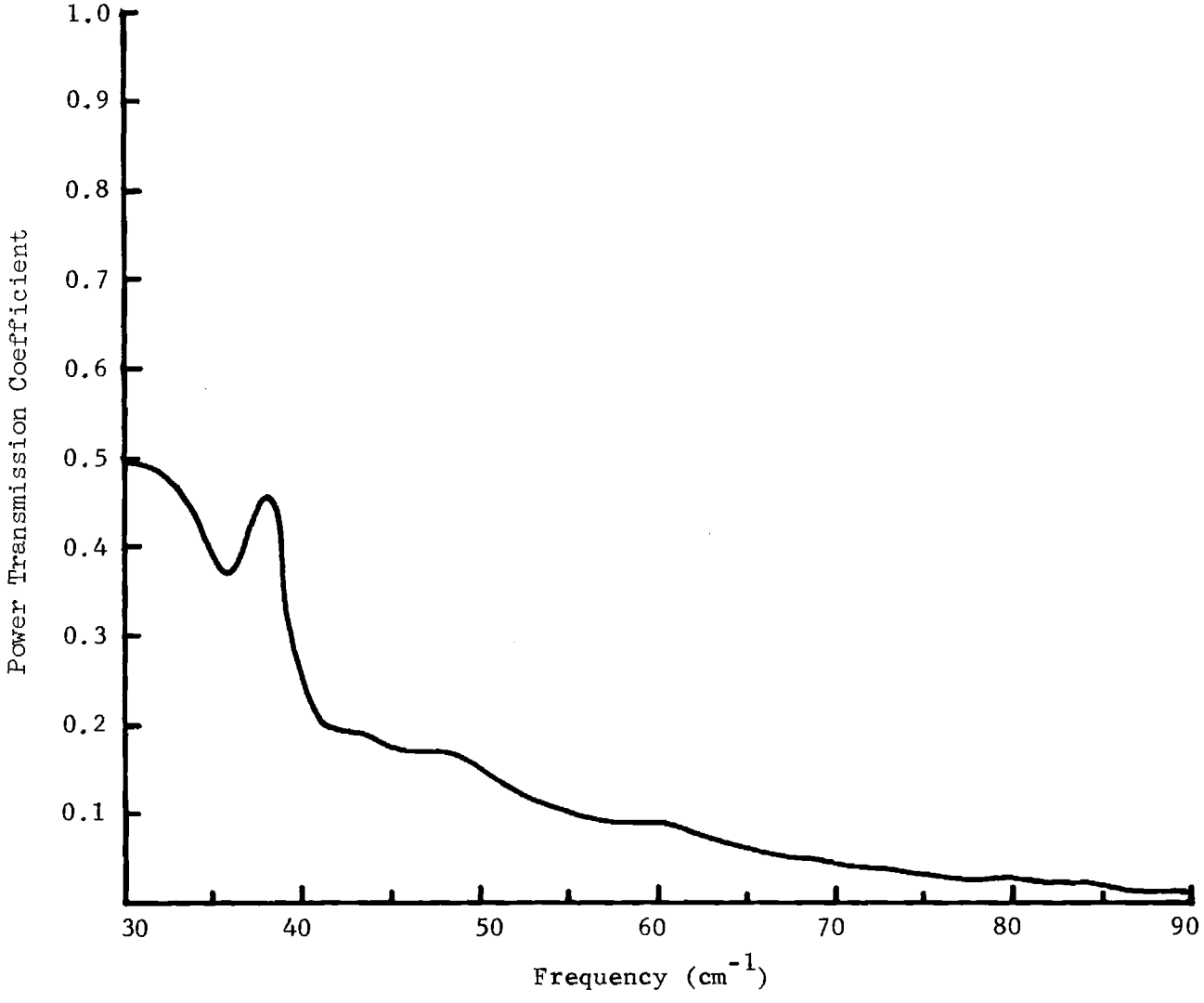

Figure 10. Power Transmission Coefficient for 0.1239" thick Dynasil Fused Silica Sample

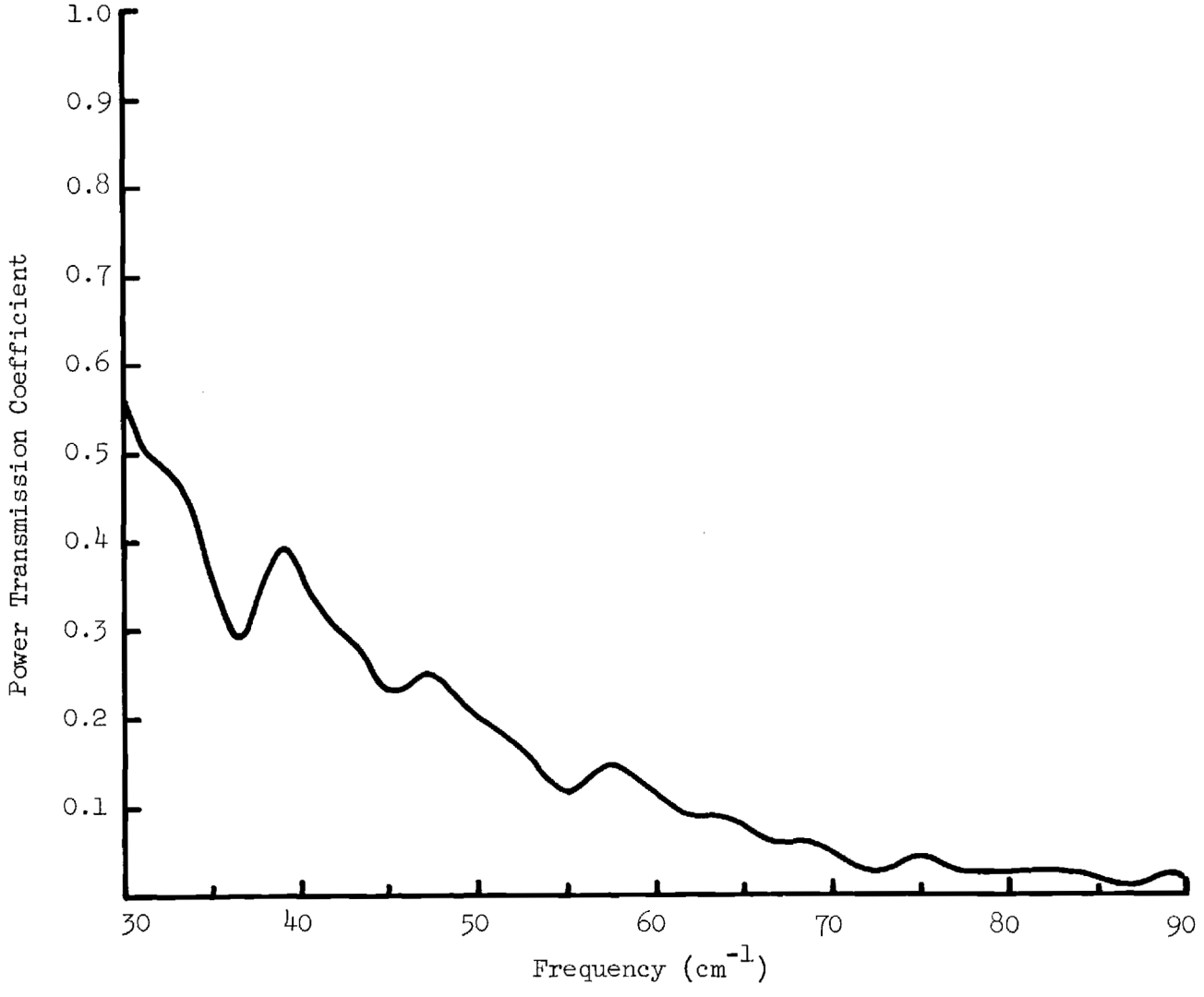

Figure 11. Power Transmission Coefficient for 0.1258" Amersil Fused Silica Sample

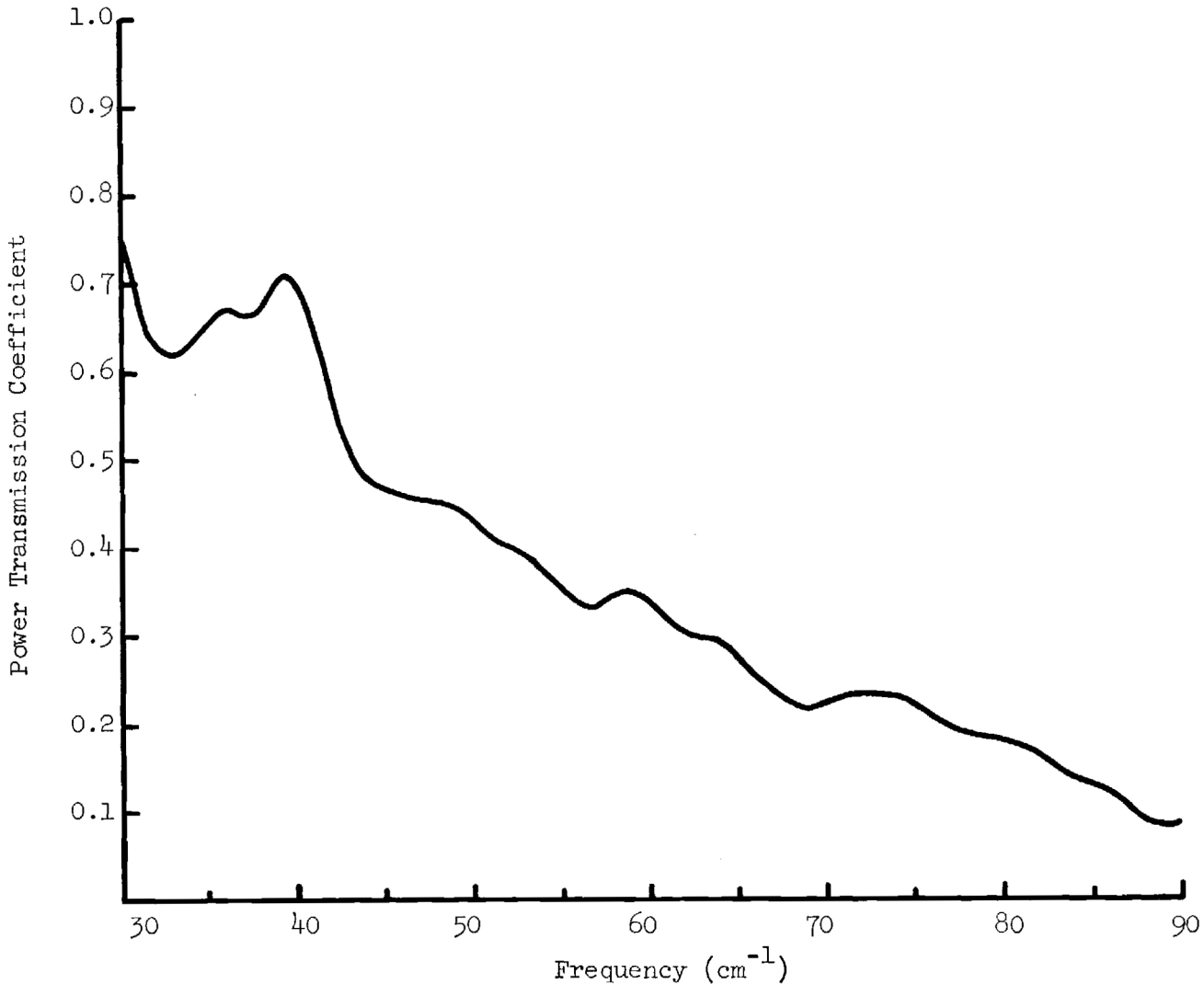

Figure 12. Power Transmission Coefficient for 0.0615" thick General Electric 102 Quartz Sample

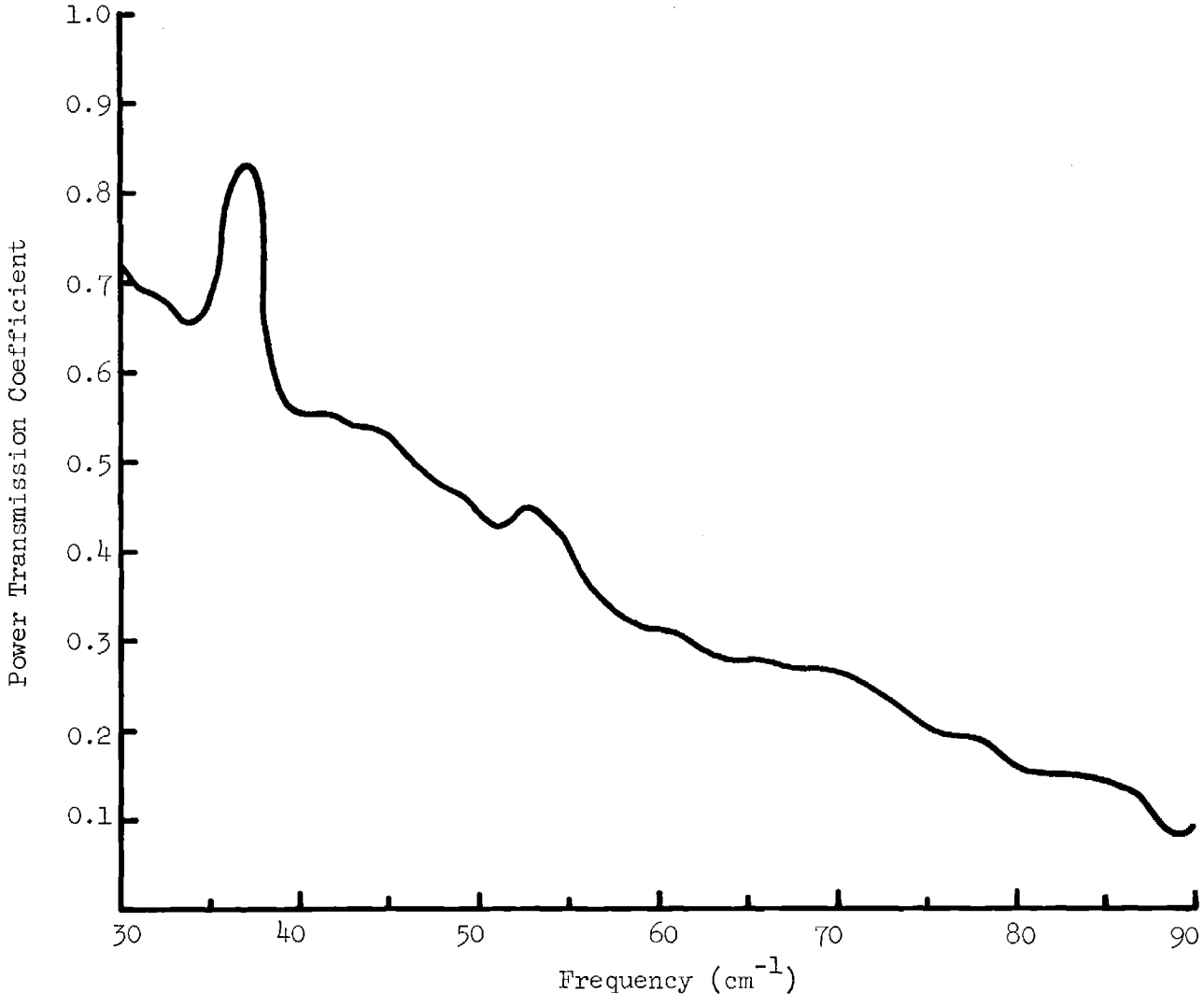

Figure 13. Power Transmission Coefficient for 0.0580" thick General Electric 101 Quartz Sample

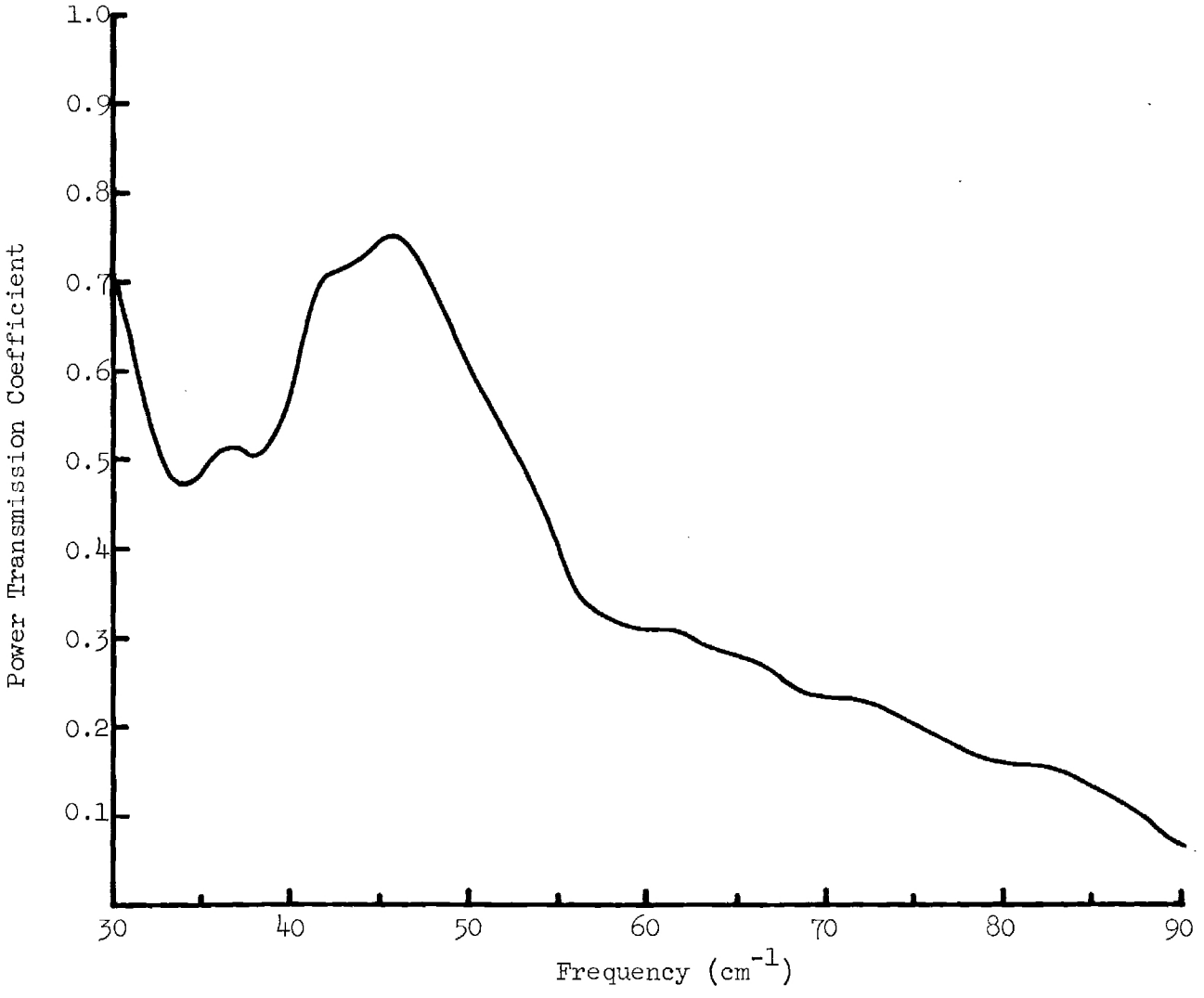

Figure 14. Power Transmission Coefficient for 0.0033" thick Mica Sample

Appendix E discusses how powdered samples can be used to measure dielectric constant in small waveguide which is available at frequencies to 325 GHz (10.8 cm^{-1}). Powdered samples eliminate the difficult problem of getting an accurately machined sample to fit in a waveguide perhaps no larger than 0.43 x 0.86 mm rectangular cross section.

In Appendix F the potential of the Fabry-Perot cavity is demonstrated for measurement of dielectric constant and loss tangent. Fabry-Perot cavities are utilized from the microwave region through the optical region so the basic technique has applicability over this entire spectral range. Experimental verification of this technique was obtained at 94 GHz (3.1 cm^{-1}).

V. Conclusions

Interference spectroscopy and free-space coherent techniques can be used to measure dielectric constant, loss tangent and transmission coefficient in the submillimeter wave region. Many materials commonly employed in the microwave region of the spectrum tend to be very lossy as a function of increasing frequency toward 2000 GHz (67 cm^{-1}). Some materials, however, such as Teflon, polyethylene, Rexolite, and slip-cast fused silica have sufficiently low dissipation factors as to represent excellent candidates for component and electromagnetic window applications throughout this part of the spectrum.

VI. REFERENCES

1. H. A. Gebbie, F. D. Findlay, et al., Nature 202, 169 (1964)

2. F. J. Low, JOSA 51, 1300 (1961)

3. K. H. Breeden and A. P. Sheppard, Technical Report No. 1, Office of Naval Research Contract Nonr-991(13), AD 644523, (17 Nov 1966)

4. R. Ulrich, K. F. Renk, and L. Genzel, IEEE Trans. MTT, 11, No. 5, 363 (September 1963)

APPENDICES

APPENDIX A

"Millimeter and Submillimeter
Wave Dielectric Measurements"

Microwave Journal
(November, 1967)

TECHNICAL SECTION

MILLIMETER AND SUBMILLIMETER WAVE DIELECTRIC MEASUREMENTS*

K. H. Breeden and A. P. Sheppard
Engineering Experiment Station
Georgia Institute of Technology
Atlanta, Georgia

Appendix A

INTRODUCTION

The extension of the electromagnetic spectrum through the microwave region and into the millimeter wave region has meant that the dielectric properties of solid materials have become increasingly important at higher and higher frequencies to both the solid-state physicist and to the systems engineer. Dielectric constant and loss tangent for many materials of interest have been measured and tabulated from dc to wavelengths in the centimeter range. Also, comprehensive data exists for materials of use in the optical and near infrared region of the spectrum. There seem, however, to have been few measurements made in the millimeter and submillimeter wave part of the spectrum.

The purpose of this paper is to show how some well-known principles used in optical/infrared technology can be used with some equally basic techniques common to microwave physics in order to obtain dielectric constant and loss tangent data in the 30 - 3000 GHz frequency region. The techniques to be described here are implemented with a Michelson-type interference spectrometer and avoid some of the problems normally encountered in materials measurements in this region, including the need for a coherent source, exceedingly small samples and waveguide transmission systems. Data will be presented for frequencies near 70 GHz and 400 GHz to illustrate the utility of the method for measuring the complex permittivity of some fairly common dielectrics which are often employed in the microwave region. It is hoped that these data will be of interest to engineers considering problems of system design in the millimeter and submillimeter region.

SUMMARY OF THE INTERFERENCE SPECTROMETER OPERATION

In order to illustrate how the Michelson interferometer may be used in dielectric measurements, a brief review of its operation is presented. The most important property of this interferometer is that radiation emitted from a broadband noise source is divided into two paths of variable length and re-combined at a square-law detector whose output can be recorded as a function of the differential length in the two paths.

Fig. 1 is a schematic diagram of

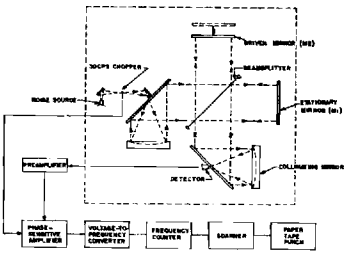

Fig. 1 — Schematic of spectrometer and block diagram of output and data recording equipment.

an interference spectrometer using a Michelson beamsplitting arrangement. The chopped noise source radiation is divided at the beamsplitter and ultimately returned from mirrors M1 and M2 to the detector. Mirror M1 is held fixed, hence giving a path length which is constant. Mirror M2 is driven at a constant speed from a reference point L_o which corresponds to zero path difference with respect to the radiation in the path of M1. The function which is obtained by recording power as a function of path difference L which is referenced from L_o is called an interferogram. It can be shown[1,2] that the power spectrum of the incoming radiation is given by the Fourier transform of the interferogram. The interferogram is normally weighted with a triangular apodizing function in order to reduce side lobes, and it can also be shown that this apodizing function limits frequency resolution to about c/L, where c is the free space velocity of light.

In addition, the instrument can be used to make conventional interferometer measurements. In this case, the phase shift introduced by inserting a sample into the path of mirror M1 is measured by displacing mirror M2. Frequency resolution in interferometer measurements is determined by the spectrum of incoming radiation and can be adjusted by filtering radiation emitted from the broadband noise source.

An instrument of the type described above has been built at Georgia Tech using a 30-cm. aperture and 2-meter effective path length. The Georgia Tech spectrometer is capable of operation from wavelengths of 8 mm. to 100 μ, with maximum resolution from 250 to 500 at these respective ends of the

* *This work was supported through Office of Naval Research Contract Nonr-991-(13).*

spectral coverage. This instrument is shown in the photograph of Fig. 2.

Fig. 2 — Photograph of the spectrometer and infrared detector.

DIELECTRIC CONSTANT MEASUREMENTS

The dielectric constant measurements to be discussed result from an extension of the interferometer technique for optical frequency measurements. A similar technique has been reported by Chamberlain, et al.[3] In measuring dielectric constant, the zero effective path difference point of mirror M2 is found by noting the position of M2 corresponding to maximum detected power. The test sample is then inserted into the path of mirror M1 and the resulting path-length change or phase shift is found by displacing mirror M2 to the new maximum power position.

The dielectric constant of a low loss material can be calculated by a derivation[4] based on the complex transmission coefficient of the material obtained by Redheffer[5] from which the phase shift introduced by inserting the sample into the beam may be expressed by

$$\Phi_s = (\beta_0 - \beta_1)d - \Phi \qquad (1)$$

where

$$\beta_0 = \frac{2\pi}{\lambda}$$

$$\beta_1 = \frac{2\pi n}{\lambda}$$

d = sample thickness

λ = free space wavelength

$n = \sqrt{\varepsilon_r}$ = index of refraction of sample

ε_r = dielectric constant of sample

$$\tan\Phi = \frac{e^{-2\alpha l}\sin 2\beta_1 d}{\left(\frac{n+1}{n-1}\right)^2 - e^{-2\alpha l}\cos 2\beta_1 d}$$

$$\alpha = \pi \tan\delta$$

and

$$l = \frac{nd}{\lambda}$$

The phase shift introduced in the path of mirror M2 by displacing it by an amount $\triangle L$ is given by $-\beta_0 \triangle L$ so the value of $\triangle L$ for maximum detected power is given by

$$(\beta_1 - \beta_0)d + \Phi = \beta_0 \triangle L$$

and

$$n = 1 + \frac{\triangle L}{d} - \frac{\Phi}{\beta_0 d} \qquad (2)$$

When the differential distance between mirrors M1 and M2 is set at the value $\triangle L$ defined by Equation (2), the fields reflected from mirrors M1 and M2 add in phase at the detector. If the distance from the sample to mirror M1 is large, the reflections from the dielectric differ in phase by a fairly large path delay when compared with the reflection from mirror M2. Thus, when radiation emitted from the source is distributed over a fairly wide frequency band, the fringes resulting from the interface reflections are negligible compared with the central fringe and the location of the central fringe is consequently determined by Equation (2).

If the term $\Phi/\beta_0 d$ is neglected, Equation (2) reduces to

$$\varepsilon_r \simeq \left(1 + \frac{\triangle L}{d}\right)^2 \qquad (3)$$

and the error in Equation (3) is determined by the angle $\theta = \Phi/\beta_0 d$. For reasonably small dielectric constant, the quantity $A = (n+1)^2/(n-1)^2$ plotted in Fig. 3 is large and the expression for Φ can be approximated by

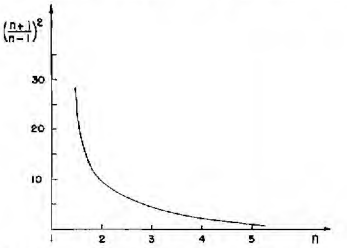

Fig. 3 — Curve showing sensitivity of dielectric constant calculation to increasing values of refractive index.

$$\Phi \simeq \frac{e^{-2\alpha l}\sin 2\beta_1 d}{A} \qquad (4)$$

The phase error θ is, therefore, limited by the inequality

$$|\theta| < \frac{1}{\beta_0' A d} \qquad (5)$$

where β_0' is the value of β_0 corresponding to the longest wavelength of radiation emitted by the source. Neglecting the phase error θ is equivalent to assuming a dielectric material of infinite thickness and consequently neglecting interface reflections. Errors introduced by the above expression are, therefore, referred to as finite thickness errors in the remainder of this paper.

The data for a dielectric constant measurement is recorded by first indexing a position on the drive of mirror M2, then driving M2 through the central maximum with no sample inserted in the beam. The traverse is then moved back to the indexed position, the sample to be tested is inserted in the path of M1 and mirror M2 is again driven through the central maximum. The dielectric constant is computed using Equation (3) with the quantity $\triangle L$ taken as the path distance between the two maxima as shown in Fig. 4

KENNETH H. BREEDEN received a BEE and MSEE from the Georgia Institute of Technology. Currently, he is a Research Engineer at the Engineering Experiment Station of the Georgia Institute of Technology and has worked with interference spectroscopy and dielectric materials measurements at millimeter wavelengths since 1964. He is a member of Tau Beta Pi and Eta Kappa Nu.

ALBERT P. SHEPPARD received a BS in Physics from Oglethorpe College, an MS in Physics from Emory University and a PhD in Electrical Engineering from Duke University. From 1960 to 1963 Dr. Sheppard was employed as a senior engineer for the Martin Company where he worked with lasers, radiometers, and various millimeter wave projects including Fabry-Perot interferometers. In 1963 he headed the electronics basic research program for the U. S. Army Research Office-Durham. Currently, Dr. Sheppard is a senior research physicist and head of the Special Techniques Group at the Georgia Institute of Technology. He is a member of Sigma Xi and a senior member of the IEEE.

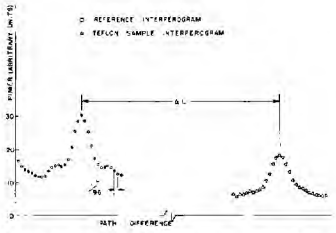

Fig. 4 — Typical interferograms for dielectric constant measurements.

and finite thickness error due to multiple reflections is calculated from Equation (5).

The above discussion assumes that dielectric constant of the sample does not vary significantly over the frequency band provided by the source and filtering for a given measurement. For the results listed in Table I, it can be seen that excursions in dielectric constant over an octave in frequency are generally within the limits of maximum error for a given measurement, so the above assumption is not unreasonable for these measurements. If, however, the dielectric constant of a material measured by the above technique is found to be drastically different from the known dielectric constant at a neighboring frequency, one would obviously be forced to use a more conventional technique such as one of the well-known coherent methods or the high-resolution power-spectrum technique discussed in Reference 2.

The results of a few recent broadband interferometer measurements for 250-450 GHz are shown in Table I along with some previously reported values.[6-8] The values listed at 71 GHz were taken from interferometer measurements using a klystron source. For these measurements, the technique is similar to the broadband technique discussed earlier, but samples are tilted at a very small angle in order to eliminate the reflected components from the dielectric/air interface. The finite thickness error, $\Phi/\beta_0 d$, is calculated using Equation (4), and this error is used to adjust the value of ε_r given by Equation (6). As a result of the above iterative process, errors in the coherent technique are limited to essentially the non-uniform thickness errors listed in Table I. The non-uniform thickness errors are taken as simply the per cent difference found in calculating dielectric constant using the nominal thickness of the sample and using the thickness corresponding to maximum excursion from the nominal value. The large errors due to non-uniform thickness of the samples could be reduced to values somewhat lower than those indicated in Table I by careful selection or lapping of the samples. Because the non-uniform thickness error can be readily calculated, the preliminary nature of these measurements dictated that other problems receive more attention than the precision finishing of samples. The improvement that would be obtained by the precise finishing can be understood by considering commercial grade polystyrene.

Polystyrene that was purchased from a plastics supplier has a thickness variation of ±0.008 inches for a 0.102-inch-thick sheet. As shown in Table I, this yields a maximum measurement error of six per cent. By lapping and repolishing the sheet, the thickness variation could be reduced to less than ±0.001 inches which would reduce the error to less than one per cent.

The 250 - 450 GHz dielectric constant measurements for plexiglass, polyethylene, and Rexolite are in fairly good agreement with the lower frequency measurements. A notable drop is seen in dielectric constant for polystyrene, pyrex, and Teflon at 250 - 450 GHz; but for pyrex the drop in dielectric constant from 4.65 at 25 GHz to 4.46 at 250 - 450 GHz is not inconsistent with the apparent behavior of pyrex at lower frequencies. The drop in dielectric constant for TTeflon and polystyrene is somewhat unexpected but the non-uniform thickness errors were 4 and 6 per cent for these samples. It might be noted that measurements reported by Chamberlain and Gebbie[9] give 1.94 as the dielectric constant of Teflon at 890 GHz using a laser source. This value agrees with the observation reported herein.

The spectral bandwidth for the interferometer measurements given in Table I is quite large. This is because only a simple black photographic filter was used to limit high frequency radiation. Work is now underway to develop more selective bandpass filters, and it is believed that the use of these filters along with uniform samples will facilitate measurements for a number of narrow frequency bands.

Table I

Dielectric Constant Values For Some Common Materials Over Frequency Range From 10 GHz - 450 GHz

	Dielectric Constant								
	(1)	(1)	(2)	(4)	(2)	(3)	(5)	(6)	(7)
Material	**10 GHz**	**25 GHz**	**70 GHz**	**71 GHz**	**139 GHz**	**343 GHz**	**250-450 GHz**	**Maximum Error**	
Fiberglass	—	—	—	4.38	—	—	4.34	< 1%	< 3%
Plexiglass	2.59	—	2.62	2.61	2.61	2.61	2.62	< 1%	< 5%
Polyethylene	2.25	2.24	—	2.28	—	2.31	2.27	< 1%	< 1%
Polystyrene	2.54	2.54	2.53	2.57	2.53	2.57	2.48	< 1%	< 6%
Pyrex	4.80	4.65	—	—	—	—	4.46	< 1%	< 3%
Rexolite	2.54	—	—	2.58	—	2.54	2.52	< 1%	< 1%
Teflon*	2.08	2.08	2.10	2.10	2.07	2.07	1.99	< 1%	< 4%

Notes:
(1) Von Hippel[8]
(2) Papolar[7]
(3) Degenford and Coleman[6]
(4) Georgia Tech coherent interferometer measurements
(5) Georgia Tech broadband interferometer measurements
(6) Finite thickness errors for Column (5) Note: Finite thickness errors for Column (4) are negligible
(7) Non-uniform thickness errors for Columns (4) and (5)

* *Interferometer measurements by Chamberlain and Gebbie[9] give 1.94 for dielectric constant of Teflon at 890 GHz.*

LOSS TANGENT

Loss tangent measurements have been made by calculating wide resolution power spectra from an interferogram recorded with no sample inserted in the beam and a second interferogram recorded with the sample inserted in the beam. The wide resolution bandwidth is used to average out the effects of multiple reflections and approximate a sample of infinite thickness.

From the derivation based on References 4 and 5, it follows that for a material of thickness d the ratio of the above two spectra is given by

$$T = |t|^2 = \frac{16n^2}{(n+1)^4 e^{2\alpha l} + (n-1)^4 e^{-2\alpha l} - 2(n^2-1)^2 \cos 4\pi l} \quad (6)$$

where $l = nd/\lambda$ and $\alpha = \pi \tan \delta$. Since α and l are always positive, $e^{2\alpha l}$ is greater than $e^{-2\alpha l}$. Also, for sufficiently small n, the term $(n+1)^4$ is much greater than $(n-1)^4$ so Equation (6) reduces to

$$T \simeq \frac{16n^2}{(n+1)^4 e^{2\alpha l} - 2(n^2-1)^2 \cos 4\pi l} \quad (7)$$

The cyclic variations introduced by the cosine term in Equation (7) increase in frequency as l is increased. Thus, if the sample is selected such that l is large and if resolution bandwidth of the power spectra is large compared to l^{-1}, then Equation (7) reduces to

$$T \simeq \frac{16n^2}{(n+1)^4} e^{-2\alpha l} \quad (8)$$

The loss tangent measurements given in Table II were calculated from transmission spectra such as the one shown in Fig. 5 using Equation (8). The graph shown in Fig. 5 shows the transmission spectrum through a 0.077-inch-thick pyrex sample. This plot and the resulting calculations shown in Table II indicate a radical increase in loss tangent for pyrex at submillimeter wavelengths. Teflon, Rexolite and polystyrene appear to have fairly low loss at frequencies as high as 1000 GHz. Reproducibility of the power spectra is known to be within a few per cent, but no error analysis has been performed on the measurements. It can be seen, however, that the solutions, in terms of $e^{2\alpha l}$ of the more exact expressions given by Equations (6) and (7) are straightforward so the ultimate limit in accuracy for loss tangent measurements is established only by reproducibility of the power spectra and by the accuracy of a prior dielectric constant measurement.

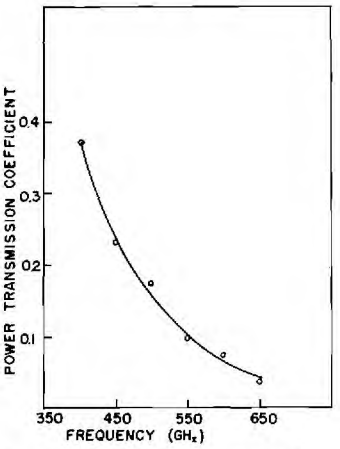

Fig. 5 — Transmission spectrum through an 0.077-inch-thick pyrex sample.

CONCLUSION

With the development of adequate bandpass filters and the use of uniform thickness materials, the interferometer dielectric measuring technique potentially offers a straightforward method for collecting data on dielectric constant of materials over the entire millimeter and submillimeter frequency band. Although this technique requires that the samples have fairly uniform thickness, the samples do have conveniently large dimensions. Thus, unlike the very small high precision samples required for high frequency waveguide measurements, these samples can easily be machined to the desired dimensions.

Results of the loss tangent measurements appear promising, but a more vigorous error analysis must be made before definitive conclusions can be made. It appears, however, that this technique will offer the capability of measuring loss tangent as a function of frequency over a band as large as 500 - 1000 GHz in a single measurement.

Table II

Loss Tangent Data For The Region From 10 GHz - 1000 GHz

	(tan δ) x 10^3						
	(1)	(1)	(2)	(2)	(3)	(3)	(3)
Material	**10 GHz**	**25 GHz**	**70 GHz**	**139 GHz**	**400 GHz**	**600 GHz**	**1000 GHz**
Pyrex	9.8	9.0			28	40	
Teflon	0.37	0.6	< 2	< 2	1	2	2
Rexolite	0.47				1	3	5
Polystyrene	0.30	0.53	0.9	2-4	3	5	7

Notes: (1) Von Hipple[8]
(2) Papolar[7]
(3) Georgia Tech spectrometer measurements

ACKNOWLEDGMENTS

The authors are grateful to Mr. Wayne K. Rivers, Jr. for his technical assistance in formulating the measurement techniques discussed above and in offering a critique of this paper.

REFERENCES

1. Rivers, W. K., "A Submillimeter Interference Spectrometer," Final Technical Report, NASA Research Grant NsG-258-62, Georgia Institute of Technology, May 8, 1964.
2. Breeden, K. H., W. K. Rivers and A. P. Sheppard, "A Submillimeter Interference Spectrometer: Characteristics, Performances and Measurements," NASA Contractor Report, NASA CR-495, May 1966.
3. Chamberlain, J. E., J. E. Gibbs and H. A. Gebbie, *Nature 198,* 1963, p. 874.
4. Breeden, K. H. and A. P. Sheppard, "Millimeter and Submillimeter Wave Dielectric Measurements with an Interference Spectrometer," Technical Report No. 1, Office of Naval Research Contract Nonr-991(13), AD 644523, Georgia Institute of Technology, November 17, 1966.
5. Redheffer, R. M., "The Measurement of Dielectric Constants," *Technique of Microwave Measurements,* New York, McGraw-Hill Book Co., 1947, pp. 561-676.
6. Degenford, J. E. and P. D. Coleman, "A Quasi-Optics Perturbation Technique for Measuring Dielectric Constants," *IEEE Proc. - 54,* No. 4, April 1966, pp. 520-522.
7. Papolar, Renaud, "Proprietes Dielectriques De Quelques Malieres Plastiques En Ondes Millimetriques," *Academie Des Sciences,* Seance Du, 1962, pp. 1763-1764.
8. Von Hipple, A., *Dielectric Materials and Applications,* The Technology Press of MIT and John Wiley & Sons, Inc., New York, 1954, pp. 291-433.
9. Chamberlain, J. E. and H. A. Gebbie, *Nature 206,* 1965, p. 602.

APPENDIX B

"A Note on the Millimeter and Submillimeter Wave Dielectric Constant and Loss Tangent Value of Some Common Materials"

Radio Science 3
(February 1968)

RADIO SCIENCE, Vol. 3 (New Series), No. 2, February 1968

A Note on the Millimeter and Submillimeter Wave Dielectric Constant and Loss Tangent Value of Some Common Materials [1]

K. H. Breeden and A. P. Sheppard

Engineering Experiment Station, Georgia Institute of Technology, Atlanta, Ga. 30332, U.S.A.

(Received July 28, 1967; revised August 18, 1967)

A tabulation of relative dielectric constant and loss tangent is presented for a number of common materials. Measurements were made by using an interference spectrometer to measure insertion loss and phase shift of dielectric samples.

2-m path, 30-cm aperture Michelson interference spectrom- has been used to measure the dielectric constant and loss gent of a number of common dielectrics in the frequency range nding from 40 GHz to 1000 GHz. The dielectric constant meas- nent technique is based on a determination of the phase shift oduced by the sample when inserted in one of the paths of the ded beam in the interference spectrometer. The loss tangent letermined by comparing the transmission coefficient obtained) and without a sample inserted in the source optical path. ails of the theory of these measurements along with results ined on Teflon and several plastics and reported elsewhere eden and Sheppard, 1967).[2] The purpose of this note is to ent a more comprehensive tabulation of results and to illus- the trend of a rather rapidly increasing loss tangent as a tion of frequency for a great many materials, with the particu- notable exception of polyethylene, which is nearly as trans- nt at 1000 GHz as it is at 10 GHz. Table 1 shows the dielectric stants that have been measured for the materials along with values reported from other sources. Table 2 shows the loss-tangent results. Figure 1 is a graph of loss tangent versus frequency from X-band to 1000 GHz. From this it may be seen that a number of dielectrics that are useful for the microwave region are essentially opaque for any reasonable thickness in the submillimeter region. The measurements program is continuing with the hope of extending the tabulations on the less lossy materials to still higher frequencies.

his work was supported through Office of Naval Research contract Nonr-991(13).

reeden, K. H., and A. P. Sheppard (1967), Millimeter and submillimeter wave dielec- measurements, Microwave J. **10**, No 12, 59–62.

LE 1. *Dielectric constant values for some common materials over frequency range from 3 GHz to 450 GHz.*

Material	Dielectric Constant (1) Microwave Frequencies	(1) 25 GHz	(4) 50 GHz	(2) 70 GHz	(4) 71 GHz	(2) 139 GHz	(3) 343 GHz	(4) 450 GHz
	1.22	.....	1.14	.....	.....	.....	.....	1.09
as Back Phenolic	.....	.....	3.11	.....	.....	.....	.....	3.33
	.....	.....	2.91	.....	.....	.....	.....	2.92
glass	.....	.....	.....	.....	4.38	.....	.....	4.34
-t Cork	.....	.....	3.42	.....	.....	.....	.....	.....
roid (NEMA G-7)	.....	.....	4.48	.....	.....	.....	.....	.....
	.....	.....	2.74	.....	.....	.....	.....	2.79
nite	.....	.....	2.62	.....	.....	.....	.....	.....
ta	4.34	.....	4.25	.....	.....	.....	.....	4.08
	3.03	.....	3.21	.....	.....	.....	.....	3.16
ite (NEMA G-10)	.....	.....	4.45	.....	.....	.....	.....	.....
Back Phenolic	.....	.....	3.41	.....	.....	.....	.....	3.37
glas	2.59	.....	.....	2.62	2.61	2.61	2.61	2.62
thylene	2.25	2.24	.....	.....	2.28	.....	2.31	2.27
tyrene	2.54	2.54	.....	2.53	2.57	2.53	2.57	2.48
	4.80	4.65	.....	.....	.....	.....	.....	4.46
ite	2.54	.....	.....	.....	2.58	.....	2.54	2.52
er Tile	.....	.....	4.65	.....	.....	.....	.....	4.35
ast Fused Silica								
1 gm/cm³)	.....	.....	3.28	.....	.....	.....	.....	.....
	2.08	2.08	.....	2.10	2.10	2.07	2.07	1.99
Asbestos Tile	.....	.....	5.33	.....	.....	.....	.....	5.25

: (1) Von Hippel, A. (1954), Dielectric Materials and Applications (The Technology Press of MIT and John Wiley & Sons, Inc., New York, N.Y.).
(2) Papoular, R. (1962), Propriétés diélectriques de quelques matières plastiques en ondes millimetriques, Compt. Rend., 1763–1764.
(3) Degenford, J. E., and P. D. Coleman (1966), A Quasi-optics perturbation technique for measuring dielectric constants, Proc. IEEE **54**, No. 4, 520–522.
(4) Georgia Tech interferometer measurements.

TABLE 2. *Loss tangent data for the region from 400 GHz to 1000 GHz*

Material	(tan δ) × 10³ 400 GHz	500 GHz	600 GHz	700 GHz	800 GHz	900 GHz	1000 GHz
Balsa	18	19	19	19	20	21	22
Canvas Back Phenolic	52	46	45	.....	.....	.....	.....
Delrin	17	20	21	23	24	24	.....
Fiberglass	41	41	43	.....	.....	.....	.....
Gasket Cork	34	42	42	.....	.....	.....	.....
Lexan	18	20	26	.....	.....	.....	.....
Nylon	16	22	26	26	.....	.....	.....
Paper Back Phenolic	37	41	41	40	39	41	.....
Plexiglas	20	20	36	.....	.....	.....	.....
Polyethylene	1.9	1.7	1.5	1.4	1.3	1.3	1.3
Polystyrene	3	.....	5	.....	.....	.....	7
Pyrex	28	.....	40	.....	.....	.....	.....
Rexolite	1	.....	3	.....	.....	.....	5
Rubber Tile	27	27	29	38	50	.....	.....
Slip-cast Fused Silica	1.7	2.7	3.6	5.1	5.9	6.2	6.4
Teflon	1	.....	2	.....	.....	.....	2
Vinyl Asbestos Tile	51	52	57	62	73	76	.....

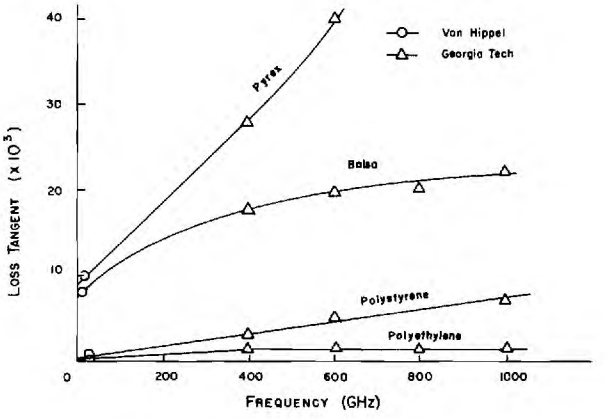

FIGURE 1. *Loss tangent as a function of frequency.*

(Paper 3–2–349)

U.S. GOVERNMENT PRINTING OFFICE : 1968 OL—279–600

APPENDIX C

"Complex Permittivity Measurements
at Millimeter Wavelengths"

Paper Accepted for
IEE Conference on:
"Dielectric Materials, Measurements and Applications"
University of Lancaster
20 - 24 July 1970

APPENDIX C

COMPLEX PERMITTIVITY MEASUREMENTS AT MILLIMETER WAVELENGTHS

K. H. Breeden, J. B. Langley, and A. P. Sheppard

A free-space waveguide bridge, an interference spectrometer, and a semiconfocal Fabry-Perot cavity have been used to measure complex permittivity of low loss dielectric materials at millimeter and submillimeter wavelengths. Frequencies for the above measurements include 50, 70, 94, 140, 850, and 1300 GHz. The materials measured include a wide selection of ceramic materials whose dielectric properties were measured at temperatures up to 1500°F and a number of organic materials such as Rexolite 1422, polystyrene, polyethylene and Teflon. Also, recent transmission coefficient measurements have been made for materials including sapphire, Irtran II, and mica at frequencies up to 6000 GHz (200 cm^{-1}).

COMPLEX PERMITTIVITY MEASUREMENTS AT MILLIMETER WAVELENGTHS*

K. H. Breeden, J. B. Langley, and A. P. Sheppard

A free-space waveguide bridge, an interference spectrometer, and a semiconfocal Fabry-Perot cavity have been used to measure complex permittivity of low loss dielectric materials at millimeter and submillimeter wavelengths. Frequencies for the above measurements include 50, 70, 94, 140, 850, and 1300 GHz. The materials measured include a wide selection of ceramic materials whose dielectric properties were measured at temperatures up to 1500°F and a number of organic materials such as Rexolite 1422, polystyrene, polyethylene and Teflon. Also, recent transmission coefficient measurements have been made for materials including sapphire, Irtran II, and mica at frequencies up to 6000 GHz (200 cm^{-1}).

In applying the waveguide bridge technique, the sample was mounted between two horns in one section of the bridge, while a precision rotary vane phaseshifter and attenuator in the other section of the bridge were used to measure insertion phase delay and insertion loss of the sample. The dielectric sample was mounted at an angle near Brewster's angle in order to minimize reflective losses and coupling between the horns and the sample. Water cooled, stainless steel horns mounted within an oven were used to illuminate the sample. The ceramic samples were heated to 1500°F and the organic materials to 350°F. Temperature profiles taken on the sample mounted inside the cylindrical oven indicate variations of less than 50°F at 1500°F.

Among the ceramic materials investigated were three fused silicas: Corning 7940, Corning 7941, and a sample of 85% density slip-cast fused silica. Also measured were samples of Pyroceram®, Rayceram III®, and alumina. The organic samples measured include Rexolite®, a fiberglass-epoxy resin laminate, and a fiberglass-polyimide resin laminate. A typical plot of loss tangent and relative dielectric constant vs. temperature for 85% density slip-cast fused silica is shown in Figure 1.

An error analysis for the equations used in calculation of loss tangent and dielectric constant was done by deriving the exact expression for dielectric constant and loss tangent and comparing these with the commonly used approximations. The approximations become essentially exact at Brewster's angle; thus, the difference represents an error term as a function of incidence angle. These errors have been calculated and graphed for each of the materials measured. Figure 2 shows a pair of relative dielectric constant and loss tangent error curves for the 85% density slip-cast fused silica sample mentioned previously.

The cavity technique applied here employed the use of a resonator in which the sample was mounted against the flat mirror in a semiconfocal system. The analysis is straight-forward and allows for the

*Research reported herein was supported in part by U. S. Navy Contract Nonr-991(13)

Georgia Institute of Technology, Atlanta, Georgia, U.S.A.

calculations of both relative dielectric constant and loss tangent from measurements of the change in cavity Q and the change in the effective length of the cavity due to insertion of the test sample. A significant advantage in this technique over previously reported cavity techniques is that placing the sample against the flat mirror in the cavity eliminates uncertainty in the angular position of the sample.

Initial measurements, using the cavity, were performed on a sample of slip-cast fused silica. The experimental data yielded the results shown in Table I.

TABLE I

MEASURED VALUES OF RELATIVE DIELECTRIC CONSTANT AND LOSS TANGENT OF SLIP-CAST FUSED SILICA

λ (mm)	F (GHz)	n	ϵ_r	tan δ
3.17	94.64	1.808	3.269	0.00259
3.18	94.34	1.814	3.292	0.00257
3.18	94.34	1.812	3.285	0.00264

Work is now underway to measure properties of several other dielectric materials with this instrument to establish further its accuracy, and to provide needed data on the millimeter wavelength loss tangents of dielectric materials.

Additional measurements have been made with a 12-inch aperture Michelson interference spectrometer. This spectrometer uses a Mylar beamsplitter whose thickness is selected for the desired measurement frequency band and a liquid helium cooled germanium detector. In making relative dielectric constant measurements, the instrument is operated in an interferometer mode with the sample mounted in the fixed path of the interferometer while insertion phase delay is measured by moving the variable mirror the distance required to equalize the two effective path lengths. Loss tangent is calculated from transmission coefficient data measured by comparing a reference power spectrum with a spectrum which is calculated from an interferogram recorded with the sample mounted in the beam of incoming radiation.

Using the above two techniques, the interference spectrometer has been used to measure relative dielectric constant and loss tangent at 850 and 1300 GHz. Measured values of relative dielectric constant and loss tangent for several organic materials as well as a sample of slip-cast fused silica are shown in Table II.

The error calculations for the relative dielectric constant values shown in Table II are based on errors due to non-uniform thickness of the samples as well as errors due to reflections at the air/dielectric interfaces.

TABLE II

MEASURED VALUES OF DIELECTRIC CONSTANT AND LOSS TANGENT AT 850 AND 1300 GHz

Material	ϵ_r		tan δ	
	850 GHz	1300 GHz	850 GHz	1300 GHz
Custom Poly,QSM	2.54 ± 0.03	2.53 ± 0.02	.003	.003
Delrin	2.80 ± 0.05	2.78 ± 0.06	.010	.010
Polyethylene	2.333 ± 0.003	2.335 ± 0.007	.0004	.0005
Polystyrene	2.520 ± 0.100	2.531 ± 0.097	.0009	.002
Rexolite 1422	2.525 ± 0.012	2.520 ± 0.009	.003	.003
SCFS 1.91 gm/cm^3	3.275 ± 0.032	3.269 ± 0.032	.003	.003
Teflon	2.042 ± 0.008	2.033 ± 0.009	.0007	.0004

Also, recent insertion loss measurements have been made for materials including sapphire, Irtran II, and mica at frequencies up to 6000 GHz (200 cm^{-1}). Although these measurements do not provide sufficient data for the calculation of relative dielectric constant and loss tangent, they provide useful transmission data for evaluating candidate far infrared "window" materials.

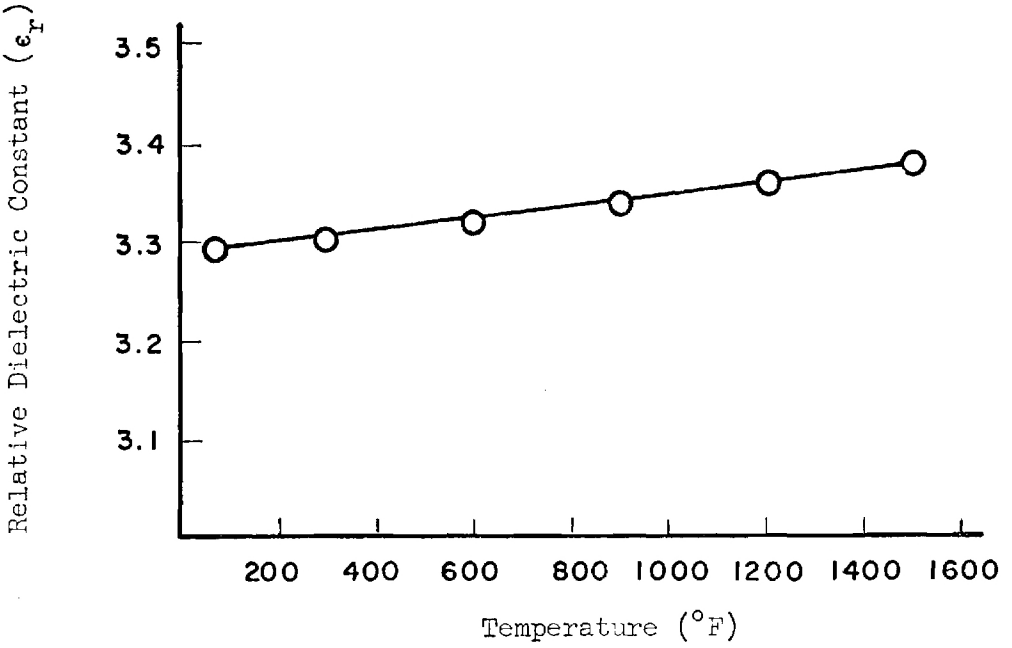

(a)

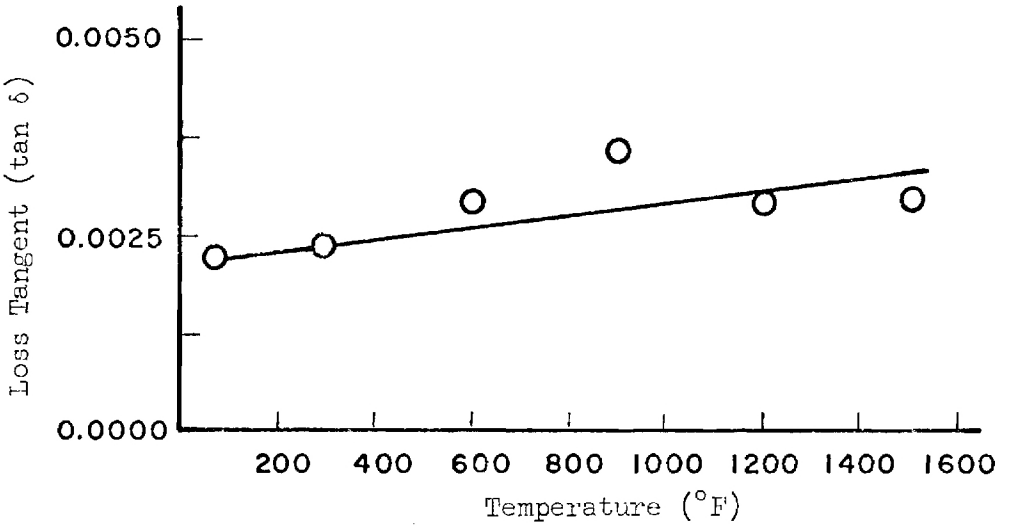

(b)

Figure 1. Complex Permittivity of 85% Density Slip-Cast Fused Silica at 94 GHz (a) Relative Dielectric Constant (b) Loss Tangent

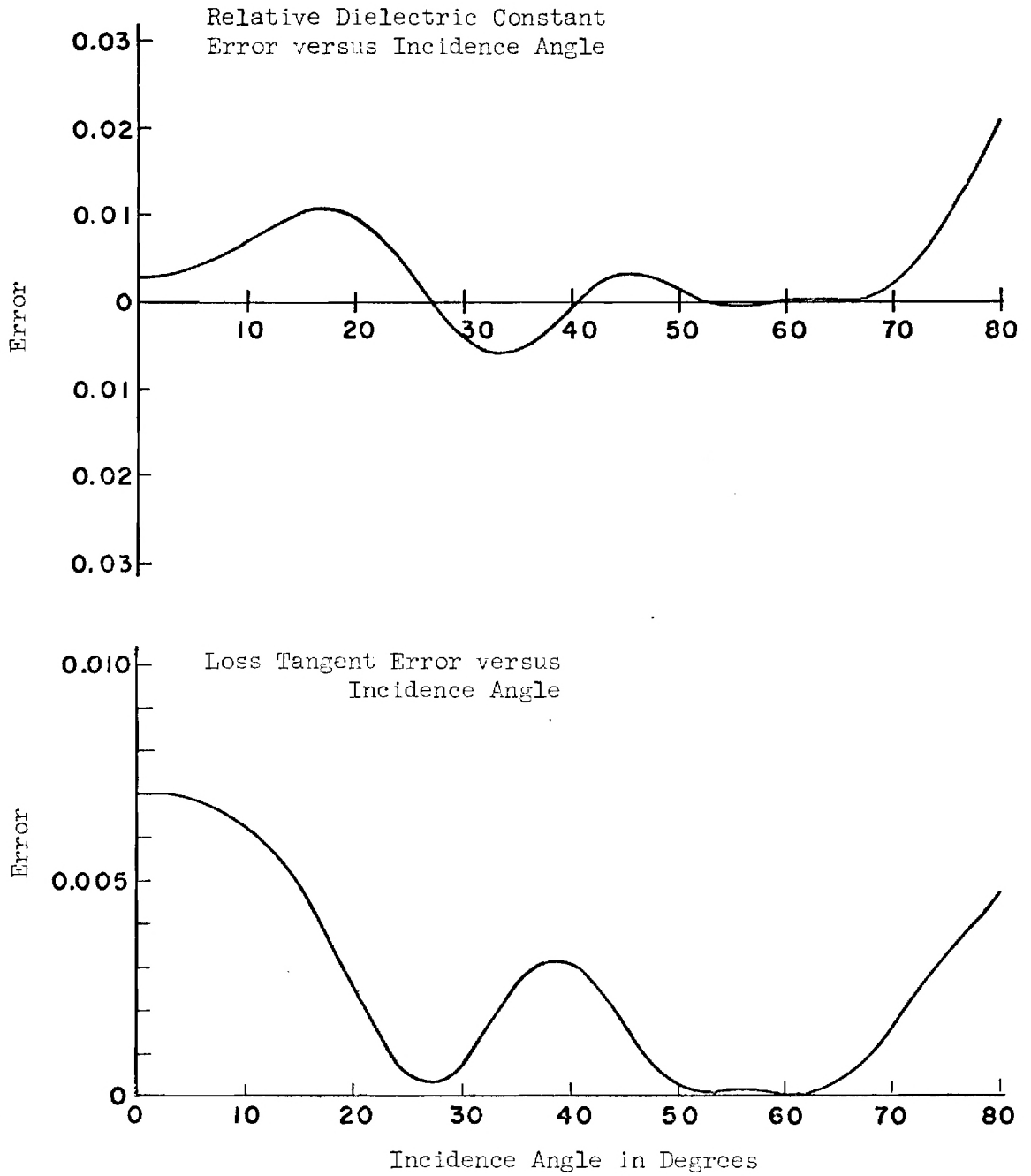

Figure 2. Predicted Measurement Error Curves for 85% SCFS, Frequency 94 GHz, Relative Dielectric Constant 3.296, Loss Tangent 0.00200, Sample Thickness 12.700 mm.

APPENDIX D

"Submillimeter Wave Material Properties
and Techniques: Dielectric Constant,
Loss Tangent, and Transmission Coefficients
of Some Common Materials to 2000 GHz"

Paper Presented to:

Polytechnic Institute of Brooklyn
Symposium on Submillimeter Waves
31 March, 1-2 April 1970

APPENDIX D

SUBMILLIMETER WAVE MATERIAL PROPERTIES AND TECHNIQUES: DIELECTRIC CONSTANT, LOSS TANGENT, AND TRANSMISSION COEFFICIENTS OF SOME COMMON MATERIALS TO 2000 GHZ*

by A. P. Sheppard, A. McSweeney and K. H. Breeden
Georgia Institute of Technology
Atlanta, Georgia 30332

A submillimeter wave interference spectrometer has been used to measure dielectric constant, loss tangent, and transmission coefficient of a number of common "window" materials at frequencies of 450, 850, 1300 and 2000 GHz. The details of the complex permittivity measurement procedure and associated mathematics have been presented elsewhere [1]. Briefly reviewed, the technique consists of using a blazed grating to isolate a relatively narrow portion of the submillimeter spectrum, for example, a 3 dB bandwidth of about 150 GHz centered at 1320 GHz, and then of measuring the phase shift introduced by insertion of a dielectric sample into the moving arm of the spectrometer. Figure 1 shows the interferogram from such a measurement on polyethylene at a center frequency of 840 GHz (28 cm^{-1}). The dielectric constant is then calculated from

$$\epsilon_r \simeq \left(1 + \frac{\Delta L}{d}\right)^2 \qquad (1)$$

where ΔL = shift in central maximum differential distance caused by sample insertion in optical path of the driven mirror

d = sample thickness.

*Supported by Office of Naval Research under Contract Nonr-991(13)

Submillimeter Permittivity Measurements

Loss tangent data is obtained by comparing the reference power spectrum with the power spectrum obtained by inserting the dielectric sample in the optical path between the grating and spectrometer input optics. From these two spectra, the transmission coefficient is calculated, and the loss tangent determined from the equation

$$T \simeq \frac{16n^2}{(n+1)^4} \exp(-2\alpha\ell) \qquad (2)$$

where T = transmission coefficient

$n = \sqrt{\varepsilon_r}$

$\ell = \frac{nd}{\lambda}$

λ = grating center wavelength

$\alpha = \pi \tan \delta$

$\tan \delta$ = loss tangent of material

Table I shows dielectric constant data and Table II shows loss tangent data for a number of materials commonly used in the microwave portion of the spectrum. In most of the data shown, there is only a small change noted in the dielectric constant whereas loss tangent generally shows an increase with increasing frequency.

Because of the 30 cm aperture of the spectrometer, fairly large diameter samples (> 10 cm) are required for the dielectric constant measurements. As seen in Equation (2), the dielectric constant calculation is also necessary for the loss tangent calculation. Several materials of interest were obtained in small diameters, and only transmission coefficients were measured as shown in Figures 2 and 3 for Irtran-2 and sapphire, respectively. These curves

demonstrate the increasing losses as a function of increasing frequency common to many materials. Larger diameters of these samples would permit calculation of the complex permittivity.

One material that has found wide application in radioastronomy is black polyethylene. Figure 4 shows that the excellent transmission properties shown in the microwave and millimeter wave region also extend into the submillimeter wave region. In this curve, there is a fair amount of instrument noise but the average transmission coefficient appears to be about 85 per cent or better from 900 GHz to 2500 GHz.

REFERENCE

1. K. H. Breeden and A. P. Sheppard, Microwave J. 10, 12, p. 59-62 (1967).

TABLE I

DIELECTRIC CONSTANT FOR SOME COMMON MATERIALS
FROM 3 GHz TO 2000 GHz

MATERIAL	DIELECTRIC CONSTANT					
	FREQUENCY (GHz)					
	3 OR 10*	50 OR 70	450	850	1300	2000
POLYETHYLENE	2.25	2.28	2.27	2.33	2.34	2.34
POLYSTYRENE	2.54	----	----	2.52	2.53	----
REXOLITE 1422	2.54	2.54	2.52	2.52	2.52	2.52
TEFLON	2.10 2.08	2.10	----	2.04	2.03	2.05
SLIP CAST FUSED SILICA	3.32	3.28	----	3.28	3.27	3.31
DELRIN	----	2.91	2.92	2.80	2.78	2.80
CUSTOM POLY QSM	2.54	----	----	2.54	2.53	2.53
DYNASIL FS	3.85	----	----	----	----	3.85
NYLON	3.03	3.21	3.16			
BALSA	1.22 1.20	1.14	1.09			
PYREX	4.80	----	4.46			
PLEXIGLAS	2.59	2.61	2.62			

* VALUES REPORTED IN THE LITERATURE

TABLE II

LOSS TANGENT FOR SOME COMMON MATERIALS
FROM 3 GHz TO 2000 GHz

MATERIAL	LOSS TANGENT				
	FREQUENCY (GHz)				
	3 OR 10*	450	850	1300	2000
POLYETHYLENE	0.0004	---	0.0004	0.0005	0.001
POLYSTYRENE	0.0002	---	0.0009	0.002	-----
REXOLITE 1422	0.0005	0.001	0.003	0.003	0.006
TEFLON	0.0003	---	0.0007	0.0004	0.002
SLIP CAST FUSED SILICA	0.0008	---	0.003	0.003	0.01
DELRIN	------	---	0.010	0.010	0.03
CUSTOM POLY QSM	0.0005	---	0.003	0.003	0.009
DYNASIL FS	0.0001	---	-----	-----	0.01
NYLON	0.013	0.02	-----	----	-----
BALSA	0.010	0.02	0.02		
PYREX	0.0098	0.03	-----		
PLEXIGLAS	0.007	0.02	-----		

*VALUES REPORTED IN THE LITERATURE

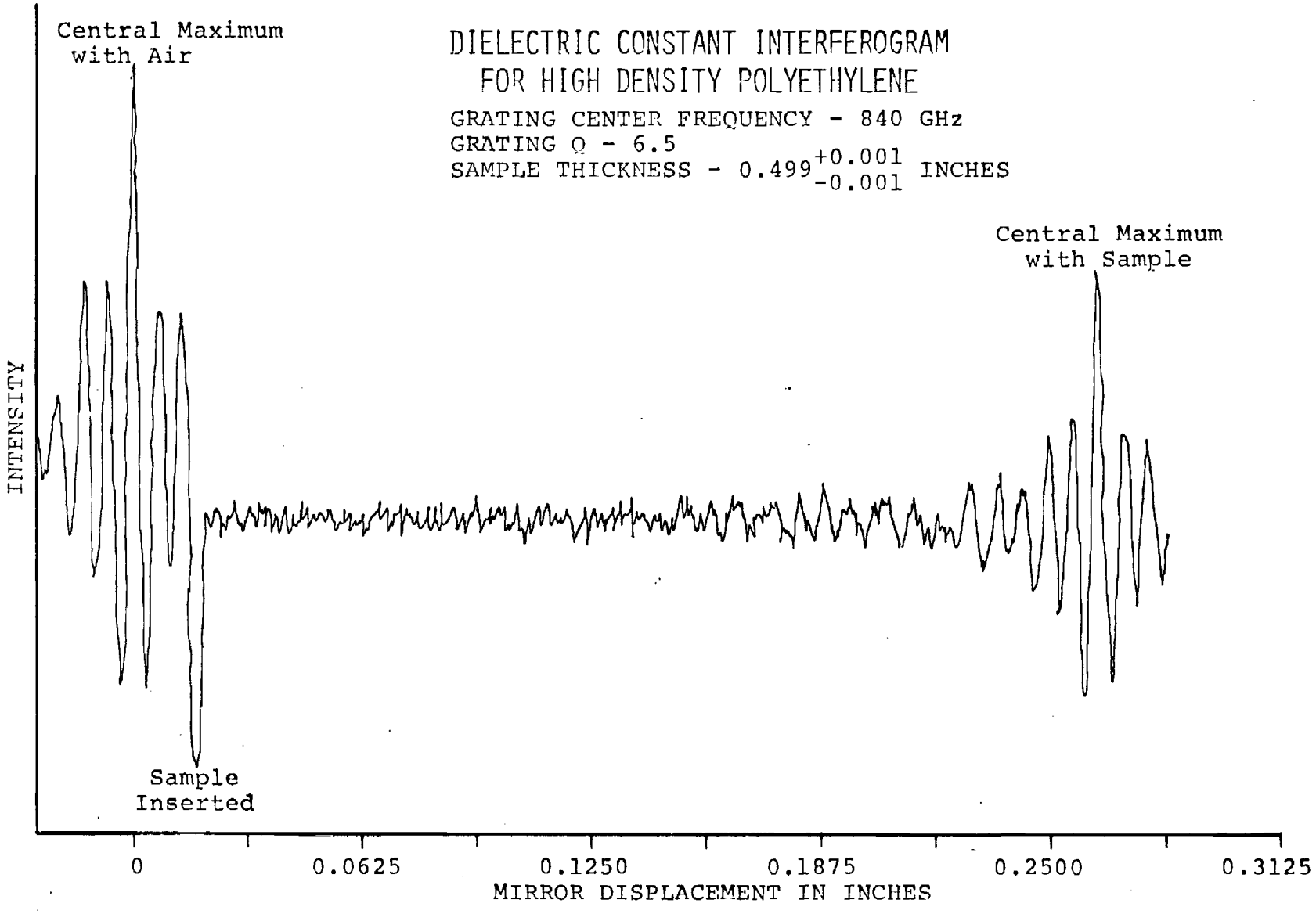

FIGURE 1. DIELECTRIC CONSTANT INTERFEROGRAM FOR HIGH DENSITY POLYETHYLENE AT 28 CM^{-1}

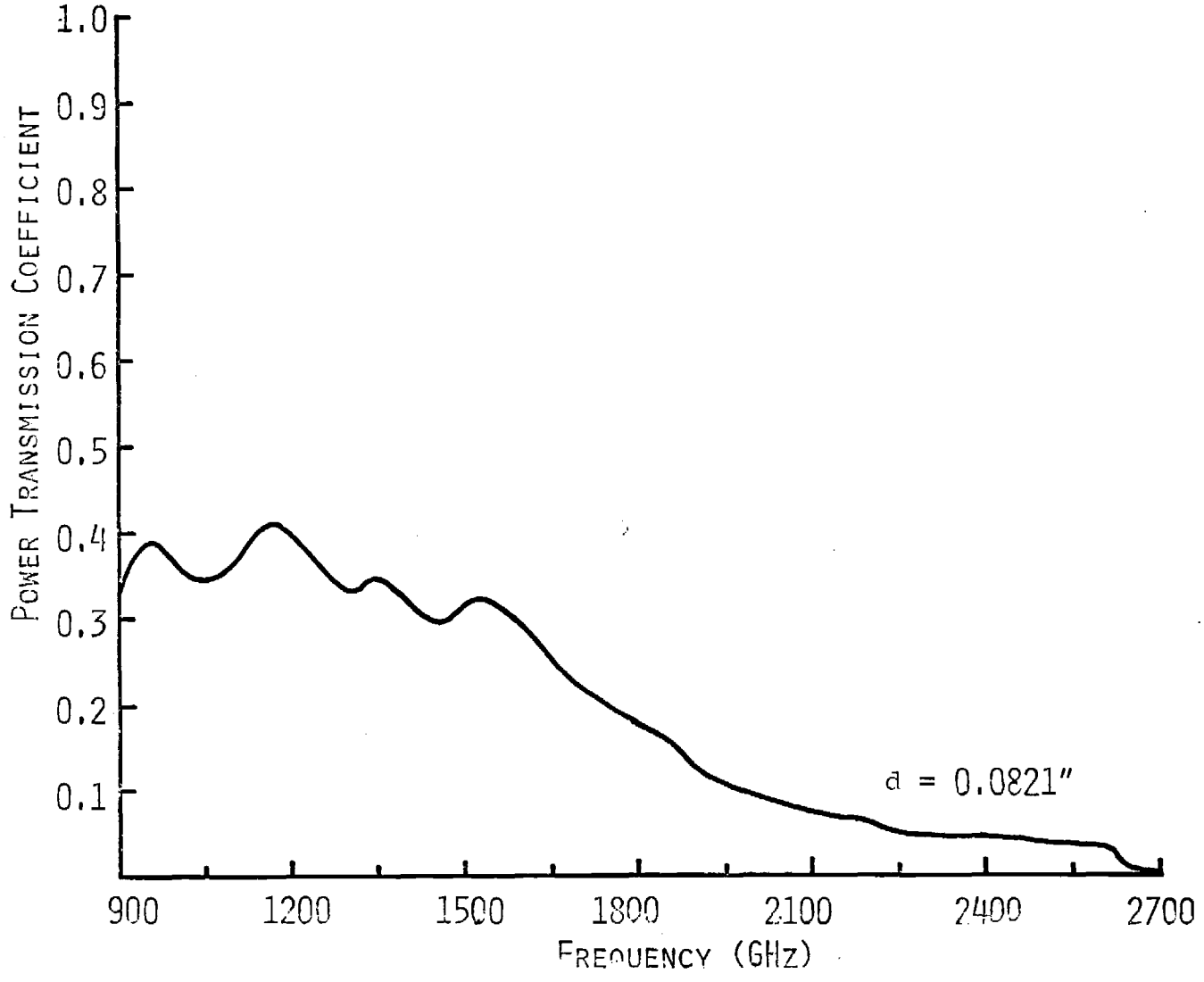

Figure 2. Power Transmission Coefficient for Irtran-2 Sample

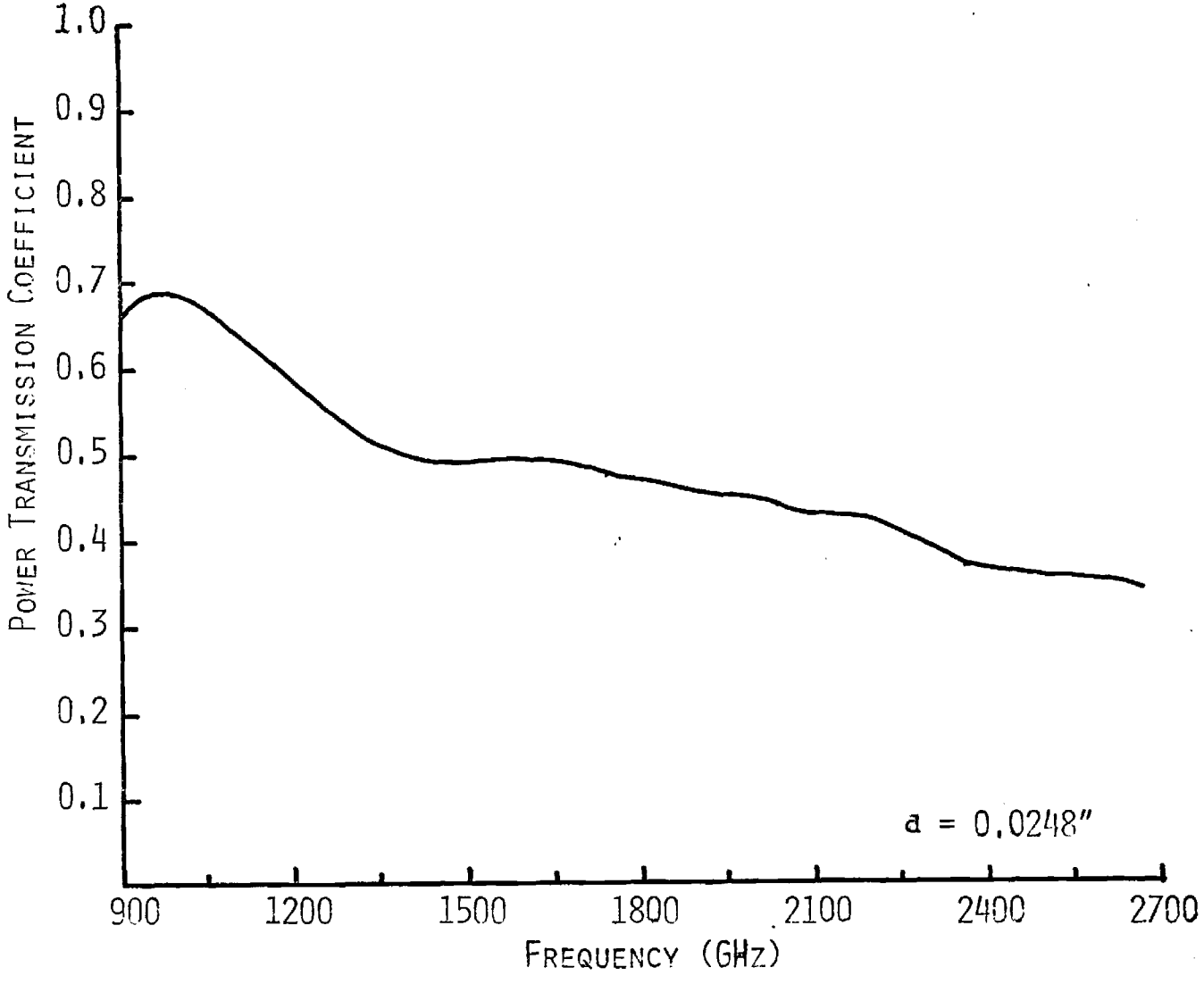

Figure 3. Power Transmission Coefficient for Sapphire Substrate

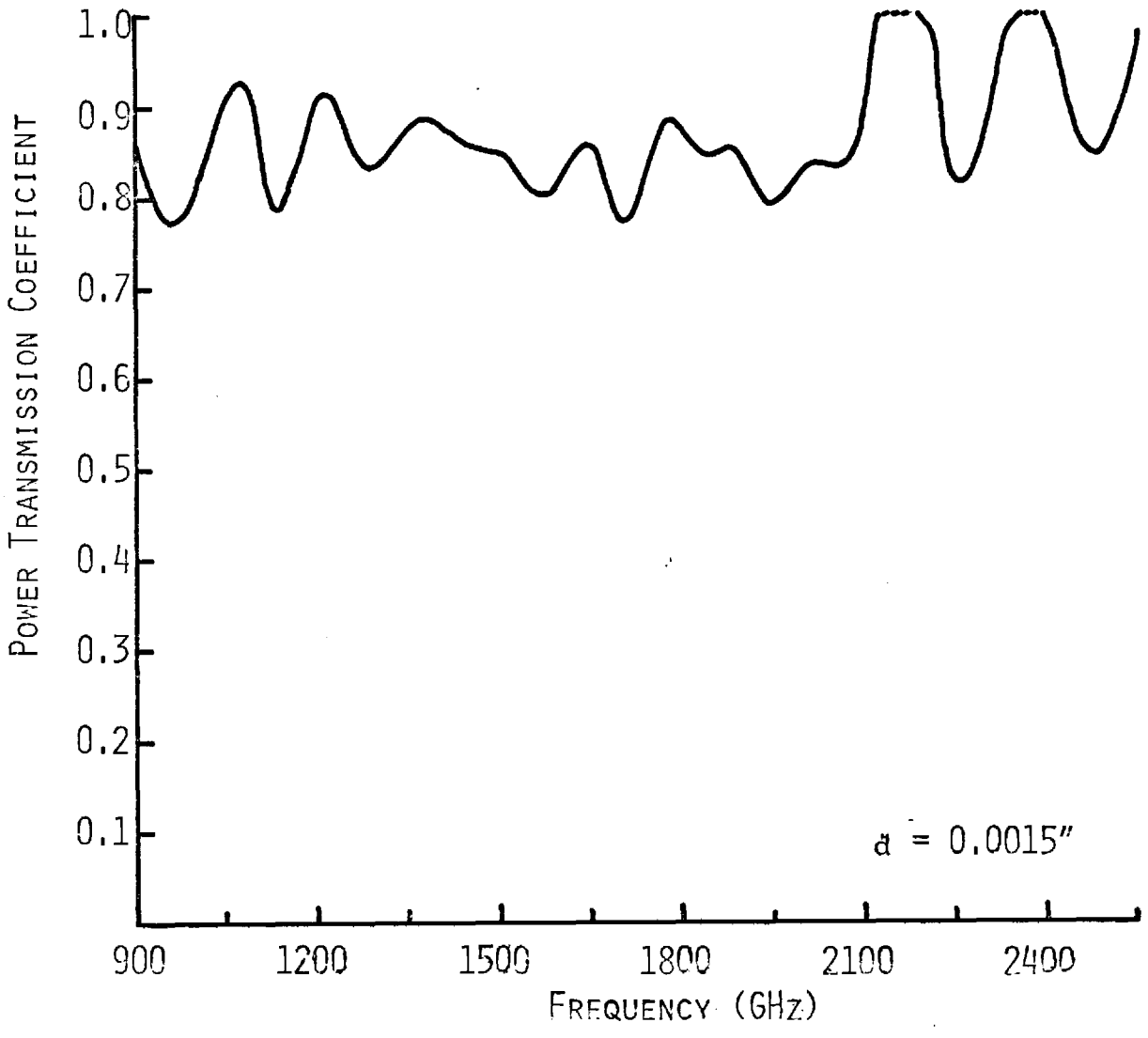

Figure 4. Power Transmission Coefficient for Black Polyethylene

APPENDIX E

"Novel Technique for Determining the Relative Permittivity of Solids at Millimetre Wavelengths"

Electronics Letters 3
(October, 1967)

NOVEL TECHNIQUE FOR DETERMINING THE RELATIVE PERMITTIVITY OF SOLIDS AT MILLIMETRE WAVELENGTHS*

A technique for determining the relative permittivity of solids from measurements made on a lower-density sample prepared from the same material is demonstrated. Data presented for three different solids at 70GHz illustrate the potential of the technique implemented with conventional short-circuit or waveguide-bridge instrumentation.

Although oscillators and detectors have recently become available in waveguide bands up to 325GHz, and microwave components are commonly available for operation at frequencies as high as 220GHz, only a limited amount of data have been published on the properties of low-loss dielectric materials at frequencies much higher than X band. It is well known that this absence of experimental data can be attributed, in part, to the extreme precision required in machining samples for conventional waveguide measurements[1] at millimetre wavelengths. Existing data at millimetre wavelengths, therefore, have been obtained by applying free-space measurements which employ the use of spectroscopy,[2, 3] interferometry,[4] or free-space cavity techniques.[5]

The purpose of this letter is to demonstrate the potential use of a dielectric measurement technique which offers the capability of using conventional short-circuit waveguide measuring techniques while avoiding the machining problems commonly associated with fabricating samples for millimetre-waveguide measurements. In implementing this measurement technique, the sample is ground into a powder, and the short waveguide section shown in Fig. 1 is used as a chamber in

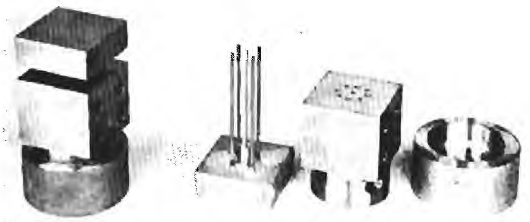

Fig. 1 *Waveguide sample holder and sample press insert*

which the powder can be pressed into pills of varying density. The waveguide chamber then serves as a sample holder in making conventional short-circuit or waveguide-bridge relative-permittivity measurements. After electrical measurements are completed, the pill is extracted and its density determined from the measured interior dimensions of the waveguide sample holder and its weight as measured on a microbalance. Thus, on measuring the relative permittivity of the sample pill at a given density ρ', the relative permittivity of the original sample material can be calculated from the following equation for the relative permittivity of materials incorporating air into the material base:[6]

$$\log \frac{\epsilon'}{\epsilon_0} = \frac{\rho'}{\rho} \log \frac{\epsilon}{\epsilon_0} \quad . \quad . \quad . \quad . \quad . \quad . \quad . \quad . \quad . \quad (1)$$

where ϵ'/ϵ_0 is the relative permittivity of the material with air, ϵ/ϵ_0 is the relative permittivity of the original solid, ρ' is the density of the material with air, and ρ is the density of the original solid.

Figs. 2*a*, *b* and *c* are plots of sample data obtained by the above measurement technique at 70GHz. Fig. 2*a* shows 'powdered' relative-permittivity data compared with theoretical data for slip-cast fused silica. The original solid material was 85% slip-cast fused silica (percentage density is based on 2·245gm/cm^3 density for 100% slip-cast fused silica). The solid-material measurement was made using waveguide-bridge measurement[7] in which the sample is placed between two horns at approximately Brewster's angle, and the insertion phase shift is measured with a precision phase shifter in the opposite arm of the bridge. The solid line shown in Fig. 2*a* was plotted from calculations using eqn. 1 and the 85% density measured point. Figs. 2*b* and *c* show similar plots for Rexolite and NEMA G-10 Panelyte. For these plots, the solid-material measurements were made using a coherent-interferometer technique.[4] It is believed that the error indicated in very low-density measured data is a result of inhomogeneity in the low-density pills. The high-density-pill measurements are, however, in very good agreement with the solid-sample measurements.

* This work was partially supported by the US Department of Agriculture Co-operative Agreement 12-14-100-9071(33) and the US Department of the Navy Office of Naval Research Contract Nonr-991(13)

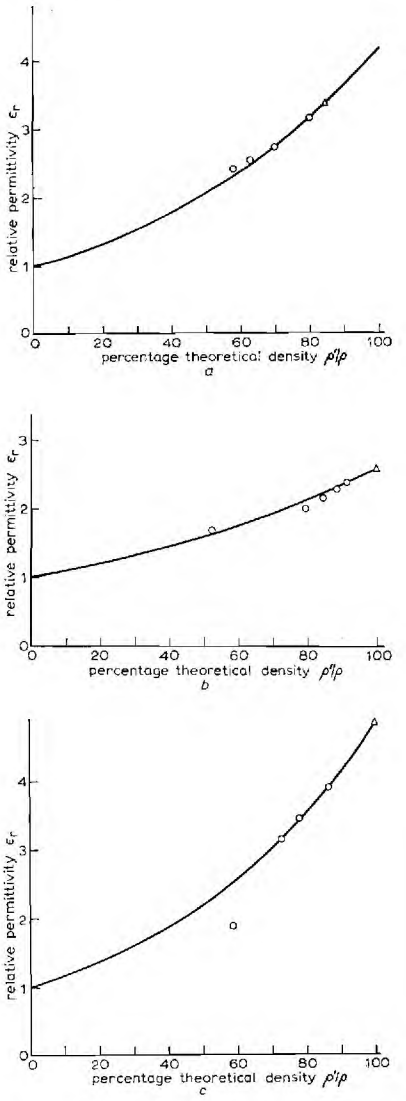

Fig. 2 *Relative permittivity against percentage theoretical density at 70GHz*

a Slip-cast fused silica
b Rexolite
c NEMA G-10 Panelyte
△ measured ϵ_r for solid sample
○ measured ϵ_r for pressed pill
—— calculated ϵ_r based on measured ϵ_r for solid sample and eqn. 1

The experimental work reported here is preliminary in nature, but is very promising in offering a permittivity-measurement technique which can be implemented easily at any frequency for which single-mode waveguide components are available. It is anticipated that future work will incorporate the use of this technique to characterise both the real and imaginary part of complex permittivity of dielectric materials.

References

1 REDHEFFER, R. M.: 'The measurement of dielectric constants', *in* MONTGOMERY, C. G. (Ed.): 'Technique of microwave measurements' (McGraw-Hill, 1947), pp. 561–676

2 BREEDEN, K. H., RIVERS, W. K., and SHEPPARD, A. P.: 'A submillimeter interference spectrometer: characteristics, performance and measurements', NASA Contractor Report, NASA CR-495, 1966

3 CHAMBERLAIN, J. E., GIBBS, J. E., and GEBBIE, H. A.: 'Refractometry in the far infra-red using a 2-beam interferometer', *Nature*, 1963,**198**, p. 874

4 BREEDEN, K. H., and SHEPPARD, A. P.: 'Millimeter and submillimeter wave dielectric measurements with an interference spectrometer', Office of Naval Research Contract Nonr-991 (13), AD 644 523, 1966

5 DEGENFORD, J. E., and COLEMAN, P. D.: 'A quasi-optics perturbation technique for measuring dielectric constants', *Proc. Inst. Elect. Electronics Engrs.*, 1966, **54**, pp. 520–522

6 KAY, A. F.: 'Radomes and absorbers', *in* JASIK, H. (Ed.): 'Antenna engineering handbook' (McGraw-Hill, 1961)

7 SHEPPARD, A. P., ABELING, A. B., and BREEDEN, K. H. *et al.*: 'Millimeter radome design techniques', Contract F33615-67-C-1243, BPSN P63416102, Interim Technical Report, 1967

APPENDIX F

"Fabry-Perot Cavity for Dielectric Measurements"

Review of Scientific Instruments 40
(September, 1969)

APPENDIX F

Reprinted from THE REVIEW OF SCIENTIFIC INSTRUMENTS, Vol. 40, No. 9, 1162-1163, September 1969
Printed in U. S. A.

Fabry–Perot Cavity for Dielectric Measurements*

K. H. BREEDEN AND J. B. LANGLEY†
Georgia Institute of Technology, Atlanta, Georgia 30332

(Received 17 March 1969; and in final form, 22 May 1969)

A technique is described for measuring complex permittivities of low loss dielectric materials with a semiconfocal Fabry–Perot resonator. Equations are derived for calculation of dielectric constant and loss tangent. Results are presented for slip-cast fused silica at 94 GHz.

A DIELECTRIC measurement technique similar to the technique reported by Degenford[1] for use with a confocal resonator has been developed for use with a semiconfocal cavity. The advantage of this technique is that it allows the simultaneous measurements of loss tangent and dielectric constant. Also, in applying this technique the sample is mounted against the flat mirror in the semiconfocal system, thus eliminating any uncertainty in the angular position of the sample. The following discussion includes a description of the measurement technique along with an outline of the derivation of equations for evaluating loss tangent and dielectric constant. Also, three sets of data for a sample of slip-cast fused silica are included to show the reproducibility of loss tangent and dielectric constant data.

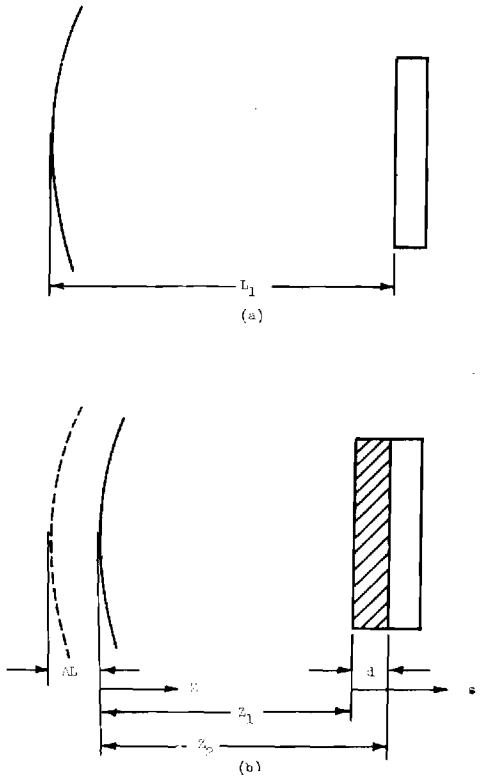

FIG. 1. Schematic diagrams for semiconfocal resonator; (a) without dielectric sample and (b) with dielectric sample.

Equations for calculating the index of refraction are derived for the semiconfocal resonator. This derivation is not conveniently achieved in the full confocal case due to the increased complexity of the field equations. The loss tangent analysis for the semiconfocal resonator is similar to Degenford's confocal resonator analysis with appropriate modifications to the boundary conditions.

If we consider the cavity geometry as shown in Figs. 1(a) and (b) in which Fig. 1(a) represents the original cavity and 1(b) the cavity with the dielectric sample placed at the plane mirror, and apply the relations of Culshaw[2] for the field equations in the cavity,

$$\left.\begin{aligned} E_0&=2A_0\sin\beta \\ Z_0H_0&=-j2A_0\cos\beta z \end{aligned}\right\} 0\leqq z\leqq Z_1$$
$$\left.\begin{aligned} E_1&=2A_1\sin(n\beta s+\psi) \\ Z_1H_1&=-j2A_1\cos(n\beta s+\psi) \end{aligned}\right\} 0\leqq s\leqq d, \tag{1}$$

where n=index of refraction of dielectric, along with an application of boundary conditions,

$$\begin{aligned} E_0(Z_1)&=E_1(0) \\ H_0(Z_1)&=H_1(0) \end{aligned} \tag{2}$$

and resonant conditions

$$E_0(0)=E_1(d)=0, \tag{3}$$

we obtain the following equations:

$$(A_1/A_0)^2=[1+\cot^2(n\beta d)]/[1+n^2\cot^2(n\beta d)] \tag{4}$$

$$\psi=\tan^{-1}[n\tan\beta Z_1]. \tag{5}$$

Also, for resonance in the original cavity,

$$L_1=m\lambda/2;$$

thus,

$$\tan(n\beta d)/n\beta d=\pm(1/\beta d)\tan\beta(d+\Delta L), \tag{6}$$

where ΔL is the mirror displacement necessary to restore resonance after the sample is inserted into the cavity.

* This work was partially supported under Office of Naval Research Contract Nonr-991(13).

† Georgia Institute of Technology, Electronics Division.

[1] J. E. Degenford, IEEE Trans. Instrum. Meas. 17, 413 (1968).

[2] W. Culshaw and M. V. Anderson, "Measurement of Dielectric Constants and Losses with a Millimeter Wave Fabry–Perot Interferometer," NBS Rep. 6786, 19 July 1961, Boulder, Colorado.

This transcendental function can be easily solved for dex of refraction, n, by using a computer generated ble of $\tan x/x$ to solve for $n\beta d$, then using known values β and d to solve for n.

The Q of the resonator can be defined in the standard ay as

$$Q=\omega\times\text{energy stored/power lost.}$$

he energy stored may be expressed as

$$W_S=\tfrac{1}{2}\epsilon\int_V E\cdot E^*dv. \tag{7}$$

lso, the power lost is given by

$$P_L=\tfrac{1}{2}\sigma\int_{V_1} E_1\cdot E_1{}^*dV_1, \tag{8}$$

ıd the losses due to diffraction, metallic losses in the flectors, etc. may be conveniently represented as a action of the total power incident upon the surfaces

$$P_{LR}=\tfrac{1}{2}\alpha\int \mathbf{E}\times\mathbf{H}^*\cdot\mathbf{n}da. \tag{9}$$

ıus,

$$Q_0=\frac{\omega E_0}{2}\int_V E\cdot E^*dv\Big/\tfrac{1}{2}a\int \mathbf{E}\times\mathbf{H}^*\cdot\mathbf{n}da \tag{10}$$

r the Q of the unperturbed cavity, and

$$=\omega\left\{\tfrac{1}{2}\epsilon_0\int E_0\cdot E_0{}^*dV_0+\tfrac{1}{2}\epsilon_1\int E_1\cdot E_1{}^*dV_1\right\}\Big/$$
$$\tfrac{1}{2}\sigma\int E_1\cdot E_1{}^*dV+\tfrac{1}{2}\alpha\int \mathbf{E}\times\mathbf{H}^*\cdot\mathbf{n}da \tag{11}$$

r the cavity with the dielectric sample inserted.

After the indicated integrations have been performed : find

$$Q_0=2\pi L_1/\lambda\alpha$$

d

$$=\frac{Z_1}{2\epsilon_r}\left[1-\frac{\sin 2\beta Z_1}{2\beta Z_1}\right]+\left(\frac{A_1}{A_0}\right)^2\frac{d}{2}\left[1+\frac{\sin^2\psi}{2n\beta d}\right]\Big/$$
$$\frac{\alpha\lambda}{4\pi\epsilon_r}+\left(\frac{A_1}{A_0}\right)^2\frac{\tan\delta}{2}d\left[1+\frac{\sin^2\psi}{2n\beta d}\right]. \tag{12}$$

ıis can be solved for the quantity of interest, $\tan\delta$,

$$n\delta=\frac{Z_1}{2\epsilon_r}\left[1-\frac{\sin 2\beta Z_1}{2\beta Z_1}\right]\Big/Q\left(\frac{A_1}{A_0}\right)^2\frac{d}{2}\left[1+\frac{\sin 2\psi}{2n\beta d}\right]$$
$$+\frac{1}{Q}-\frac{Q}{Q_0}\left(\frac{L_1}{2\epsilon_r}\right)\Big/Q\left(\frac{A_1}{A_0}\right)^2\frac{d}{2}\left[1+\frac{\sin 2\psi}{2n\beta d}\right]. \tag{13}$$

TABLE I. Measured values for relative dielectric constant and loss tangent of slip-cast fused silica.

λ	n	ϵ_r	$\tan\delta$
3.169 mm	1.808	3.269	0.00259
3.181	1.814	3.292	0.00257
3.181	1.812	3.285	0.00264

Upon rearrangement of terms and appropriate approximations for $d>\lambda/2$

$$\tan\delta\approx\frac{1}{Q}\left\{\left[Z_1-\frac{Q}{Q_0}L_1\right]\Big/\left(\frac{A_1}{A_0}\right)^2\epsilon_r d+1\right\} \tag{14}$$

all of which are readily measurable or, in the case of $(A_1/A_0)^2$, easily calculable. If $d=\lambda/2$, the error in Eq. (14) is approximately 10% which is within experimental error for typical millimeter wavelength loss tangent measurements.

In implementing this technique, the unperturbed Q of the cavity is measured by noting the width between 3 dB points on the resonance line and then using

$$Q_0=L_1/\Delta L_1$$

where L_1 = cavity length and ΔL_1 = 3 dB width, to calculate the cavity Q. The sample is then inserted and the cavity shortened by an amount necessary to restore resonance. Since the distance the mirror is moved is small compared to the total length of the cavity, we can calculate the Q of the cavity with the sample by

$$Q=L_1/\Delta L_2$$

where L_1 = length of cavity without sample and ΔL_2 = 3 dB linewidth with sample. The amount of movement necessary to restore resonance is also noted and is used to calculate index of refraction.

Measurements were performed on a sample of slip-cast fused silica. The experimental data yielded the results shown in Table I. The values obtained are reasonable based upon lower frequency measurements.[3] The small variation in values of loss tangent is particularly encouraging since reliable loss tangent measuring techniques have not been previously available at 94 GHz. Work is now underway to measure properties of several other dielectric materials with this technique to establish further its accuracy, and to provide needed data on the millimeter wavelength loss tangents of a number of low loss dielectric materials.

[3] K. H. Breeden, "Millimeter Wave Radome Design Techniques," Air Force Avionics Laboratory, Air Force System Command, Tech. Rep. AFAL-TR-68-38, February 1968.

DISTRIBUTION LIST

Director 3
Advanced Research Projects Agency
Attn: Technical Library
The Pentagon
Washington, D.C. 20301

(ARPA-supported contracts)
Advanced Research Projects Agency 3
Attn: Lt. Col. J. MacCallum
Lynn Building
Arlington, Virginia 20301

Office of Naval Research 3
Department of the Navy
Attn: Physics Branch
Washington, D. C. 20360

Naval Research Laboratory 3
Department of the Navy
Attn: Technical Library
Washington, D. C. 20390

Commanding Officer
Naval Weapons Center
Corona Laboratories
Corona, California 91720

Office of the Director of Defense
Research and Engineering 3
Information Office Library Branch
The Pentagon
Washington, D. C. 20301

U. S. Army Research Office 2
Box CM, Duke Station
Durham, North Carolina 27706

Defense Documentation Center 30
Cameron Station
Alexandria, Virginia 22314

Director, National Bureau
of Standards
Attn: Technical Library
Washington, D. C. 20234

Commanding Officer 3
Office of Naval Research
Branch Office
219 South Dearborn Street
Chicago, Illinois 60604

San Francisco Area Office 3
Office of Naval Research
1076 Mission Street
San Francisco, California 94109

Air Force Office of
Scientific Research
Deaprtment of the Air Force
Washington, D. C. 20333

Commanding Officer 3
Office of Naval Research
Branch Office
1030 East Green Street
Pasadena, California 91101

Commanding Officer 3
Office of Naval Research
Branch Office
495 Summer Street
Boston, Massachusetts 02210

Commanding Officer 5
Office of Naval Research
Branch Office
Box 39, FPO
New York, New York 09510

Director
U. S. Army Engineering Research
and Development Laboratories
Fort Belvoir, Virginia 22060
Attn: Technical Documents Center

DISTRIBUTION LIST (Continued)

ODDR & E Advisory Group on Electron Devices 201 Varick Street New York, New York 10014	3
New York Area Office Office of Naval Research 207 West 24th Street New York, New York 10011	3

UNCLASSIFIED
Security Classification

DOCUMENT CONTROL DATA - R&D

(Security classification of title, body of abstract and indexing annotation must be entered when the overall report is classified)

1. ORIGINATING ACTIVITY *(Corporate author)*

Georgia Institute of Technology
Atlanta, Georgia 30332

2a. REPORT SECURITY CLASSIFICATION
Unclassified

2b. GROUP

3. REPORT TITLE

"Millimeter and Submillimeter Wave Dielectric Measurements with an Interference Spectrometer"

4. DESCRIPTIVE NOTES *(Type of report and inclusive dates)*
Final Report

5. AUTHOR(S) *(Last name, first name, initial)*

McSweeney, Albert; and Sheppard, Albert P.

6. REPORT DATE	7a. TOTAL NO. OF PAGES	7b. NO. OF REFS
14 April 1970	58	4

8a. CONTRACT OR GRANT NO.	9a. ORIGINATOR'S REPORT NUMBER(S)
Nonr-991(13)	Final Report
b. PROJECT NO.	A-934
c.	9b. OTHER REPORT NO(S) *(Any other numbers that may be assigned this report)*
d.	

10. AVAILABILITY/LIMITATION NOTICES

Unlimited distribution

11. SUPPLEMENTARY NOTES	12. SPONSORING MILITARY ACTIVITY
	Office of Naval Research Department of the Navy Washington, D. C. 20360

13. ABSTRACT

Dielectric constants, loss tangents, and transmission coefficients for a large number of materials have been measured in the millimeter and submillimeter wave part of the electromagnetic spectrum. Instrumentation and measurement techniques for obtaining these data are described in detail. These include interference spectroscopy using a black body source with appropriately designed filters, and coherent techniques using a Fabry-Perot interferometer or a short-circuited waveguide filled with powdered samples. The measurements show that many materials commonly employed in the microwave spectrum tend to be very lossy as a function of increasing frequencies toward 2000 GHz (67 cm^{-1}). Some materials, such as Teflon, polyethylene, Rexolite, and slip-cast fused silica, were observed to have relatively low dissipation factors so as to represent excellent candidates for component and electromagnetic window applications throughout the millimeter and submillimeter wave part of the spectrum.

DD FORM 1 JAN 64 1473

UNCLASSIFIED
Security Classification

14. KEY WORDS	LINK A		LINK B		LINK C	
	ROLE	WT	ROLE	WT	ROLE	WT
Interference Spectroscopy						
Millimeter Waves						
Submillimeter Waves						
Far Infrared Techniques						
Dielectric Constant and Loss Tangent						

INSTRUCTIONS

1. ORIGINATING ACTIVITY: Enter the name and address of the contractor, subcontractor, grantee, Department of Defense activity or other organization *(corporate author)* issuing the report.

2*a*. REPORT SECURITY CLASSIFICATION: Enter the overall security classification of the report. Indicate whether "Restricted Data" is included. Marking is to be in accordance with appropriate security regulations.

2*b*. GROUP: Automatic downgrading is specified in DoD Directive 5200.10 and Armed Forces Industrial Manual. Enter the group number. Also, when applicable, show that optional markings have been used for Group 3 and Group 4 as authorized.

3. REPORT TITLE: Enter the complete report title in all capital letters. Titles in all cases should be unclassified. If a meaningful title cannot be selected without classification, show title classification in all capitals in parenthesis immediately following the title.

4. DESCRIPTIVE NOTES: If appropriate, enter the type of report, e.g., interim, progress, summary, annual, or final. Give the inclusive dates when a specific reporting period is covered.

5. AUTHOR(S): Enter the name(s) of author(s) as shown on or in the report. Enter last name, first name, middle initial. If military, show rank and branch of service. The name of the principal author is an absolute minimum requirement.

6. REPORT DATE: Enter the date of the report as day, month, year; or month, year. If more than one date appears on the report, use date of publication.

7*a*. TOTAL NUMBER OF PAGES: The total page count should follow normal pagination procedures, i.e., enter the number of pages containing information.

7*b*. NUMBER OF REFERENCES: Enter the total number of references cited in the report.

8*a*. CONTRACT OR GRANT NUMBER: If appropriate, enter the applicable number of the contract or grant under which the report was written.

8*b*, 8*c*, & 8*d*. PROJECT NUMBER: Enter the appropriate military department identification, such as project number, subproject number, system numbers, task number, etc.

9*a*. ORIGINATOR'S REPORT NUMBER(S): Enter the official report number by which the document will be identified and controlled by the originating activity. This number must be unique to this report.

9*b*. OTHER REPORT NUMBER(S): If the report has been assigned any other report numbers *(either by the originator or by the sponsor)*, also enter this number(s).

10. AVAILABILITY/LIMITATION NOTICES: Enter any limitations on further dissemination of the report, other than those imposed by security classification, using standard statements such as:

(1) "Qualified requesters may obtain copies of this report from DDC."

(2) "Foreign announcement and dissemination of this report by DDC is not authorized."

(3) "U. S. Government agencies may obtain copies of this report directly from DDC. Other qualified DDC users shall request through _____."

(4) "U. S. military agencies may obtain copies of this report directly from DDC. Other qualified users shall request through _____."

(5) "All distribution of this report is controlled. Qualified DDC users shall request through _____."

If the report has been furnished to the Office of Technical Services, Department of Commerce, for sale to the public, indicate this fact and enter the price, if known.

11. SUPPLEMENTARY NOTES: Use for additional explanatory notes.

12. SPONSORING MILITARY ACTIVITY: Enter the name of the departmental project office or laboratory sponsoring *(paying for)* the research and development. Include address.

13. ABSTRACT: Enter an abstract giving a brief and factual summary of the document indicative of the report, even though it may also appear elsewhere in the body of the technical report. If additional space is required, a continuation sheet shall be attached.

It is highly desirable that the abstract of classified reports be unclassified. Each paragraph of the abstract shall end with an indication of the military security classification of the information in the paragraph, represented as *(TS)*, *(S)*, *(C)*, or *(U)*.

There is no limitation on the length of the abstract. However, the suggested length is from 150 to 225 words.

14. KEY WORDS: Key words are technically meaningful terms or short phrases that characterize a report and may be used as index entries for cataloging the report. Key words must be selected so that no security classification is required. Identifiers, such as equipment model designation, trade name, military project code name, geographic location, may be used as key words but will be followed by an indication of technical context. The assignment of links, rules, and weights is optional.